14. **Hayashida Y,** Nishida K, Yamato M, *et al.* Ocular surface reconstruction using autologous rabbit oral mucosal epithelial sheets fabricated ex vivo on a temperature-responsive culture surface. *Invest Ophthalmol Vis Sci* 2005;**46**:1632–9.
15. **Pellegrini G,** Dellambra E, Golisano O, *et al.* p63 identifies keratinocyte stem cells. *Proc Natl Acad Sci U S A* 2001;**98**:3156–61.
16. **Moll I,** Troyanovsky SM, Moll R. Special program of differentiation expressed in keratinocytes of human haarscheiben: an analysis of individual cytokeratin polypeptides. *J Invest Dermatol* 1993;**100**:69–76.
17. **Rheinwald JG,** Green H. Serial cultivation of strains of human epidermal keratinocytes: the formation of keratinizing colonies from single cells. *Cell* 1975;**6**:331–43.
18. **Pellegrini G,** Traverso CE, Franzi AT, *et al.* Long-term restoration of damaged corneal surfaces with autologous cultivated corneal epithelium. *Lancet* 1997;**349**:990–3.
19. **Nishida K,** Yamato M, Hayashida Y, *et al.* Functional bioengineered corneal epithelial sheet grafts from corneal stem cells expanded ex vivo on a temperature-responsive cell culture surface. *Transplantation* 2004;**77**:379–85.
20. **Kideryova L,** Lacina L, Dvorankova B, *et al.* Phenotypic characterization of human keratinocytes in coculture reveals differential effects of fibroblasts from benign fibrous histiocytoma (dermatofibroma) as compared to cells from its malignant form and to normal fibroblasts. *J Dermatol Sci* 2009;**55**:18–26.
21. **Zakaria N,** Koppen C, Van Tendeloo V, *et al.* Standardized limbal epithelial stem cell graft generation and transplantation. *Tissue Eng Part C Methods 2010*; In press. [5]
22. **Hayashi R,** Yamato M, Takayanagi H, *et al.* Validation system of tissue engineered epithelial cell sheets for corneal regenerative medicine. *Tissue Eng Part C Methods 2010*; In press. [6]
23. **Blazejewska EA,** Schlotzer-Schrehardt U, Zenkel M, *et al.* Corneal limbal microenvironment can induce transdifferentiation of hair follicle stem cells into corneal epithelial-like cells. *Stem Cells* 2009;**27**:642–52.
24. **Yokoo S,** Yamagami S, Usui T, *et al.* Human corneal epithelial equivalents for ocular surface reconstruction in a complete serum-free culture system without unknown factors. *Invest Ophthalmol Vis Sci* 2008;**49**:2438–43.
25. **Green H.** Cyclic AMP in relation to proliferation of the epidermal cell: a new view. *Cell* 1978;**15**:801–11.

Biochemical and Biophysical Research Communications 392 (2010) 311–316

Contents lists available at ScienceDirect

Biochemical and Biophysical Research Communications

journal homepage: www.elsevier.com/locate/ybbrc

Metastable primordial germ cell-like state induced from mouse embryonic stem cells by Akt activation

Noriko Yamano [a], Tohru Kimura [b,*], Shoko Watanabe-Kushima [a], Takashi Shinohara [c], Toru Nakano [a,b,*]

[a] Graduate School of Frontier Biosciences, Osaka University, 2-2 Yamada-oka, Suita, Osaka 565-0871, Japan
[b] Department of Pathology, Medical School, Osaka University, 2-2 Yamada-oka, Suita, Osaka 565-0871, Japan
[c] Department of Molecular Genetics, Graduate School of Medicine, Kyoto University, Kyoto 606-8501, Japan

ARTICLE INFO

Article history:
Received 28 December 2009
Available online 6 January 2010

Keywords:
ES cells
Primordial germ cells
Mesoderm
Akt
Cell differentiation

ABSTRACT

Specification to primordial germ cells (PGCs) is mediated by mesoderm-induction signals during gastrulation. We found that Akt activation during *in vitro* mesodermal differentiation of embryonic stem cells (ESCs) generated self-renewing spheres with differentiation states between those of ESCs and PGCs. Essential regulators for PGC specification and their downstream germ cell-specific genes were expressed in the spheres, indicating that the sphere cells had commenced differentiation to the germ lineage. However, the spheres did not proceed to spermatogenesis after transplantation into testes. Sphere cell transfer to the original feeder-free ESC cultures resulted in chaotic differentiation. In contrast, when the spheres were cultured on mouse embryonic fibroblasts or in the presence of ERK-cascade and GSK3 inhibitors, reversion to the ESC-like state was observed. These results indicate that Akt signaling promotes a novel metastable and pluripotent state that is intermediate to those of ESCs and PGCs.

Introduction

PGCs emerge from a subset of epiblast cells that migrate to the extraembryonic region on embryonic day (E) 7 during early gastrulation in mice. The expression of Blimp1, a transcription factor essential for PGC specification, commences in a few proximal epiblast cells at E6.25 [1,2]. Another transcription factor, Prdm14, which is also essential for PGC specification, is induced in PGC precursors slightly after the upregulation of Blimp1 [3]. During PGC specification, the gene expression profiles and epigenetic statuses are drastically altered by Blimp1 and Prdm14 [1,3]. Germ cell-specific genes, such as *PGC7* (also known as *Stella* and *Dppa3*) and *Dnd1*, are induced in the nascent PGCs, i.e., the PGCs that are just emerging in the extraembryonic region at E6.75–E7.0 [4]. In contrast, mesoderm-related genes are repressed, although they are transiently induced by the mesoderm-induction signals. Pluripotency-related genes, such as *Nanog* and *Sox2*, are re-activated in the nascent PGCs. PGCs undergo epigenetic reprogramming, which involves genome-wide alterations of repressive histone modification and DNA methylation patterns from E7.75 to E9.5 [5].

Although PGCs are germ line-committed cells, they can dedifferentiate into cells that have broader differentiation potential. PGCs give rise to embryonic germ (EG) cells when cultured in the presence of leukemia inhibitory factor (LIF), stem cell factor (SCF), and basic fibroblast growth factor (bFGF) [6,7]. EG cells contribute to the somatic and germ lineages after their introduction into blastocysts, whereas freshly isolated PGCs cannot perform these functions, indicating that the special culture condition reprograms the PGCs to the pluripotent state [8,9]. In addition, testicular teratomas originate from PGCs [10].

Phosphoinositide-3 kinase (PI3K) activates downstream effectors including the serine/threonine kinase Akt, while this signal is counteracted by PTEN [11]. PGC-specific deletion of PTEN and hyperactivation of Akt promote the dedifferentiation of PGCs to EG cells *in vitro* and the formation of testicular teratomas *in vivo* [12,13], indicating that PI3K/Akt signaling plays critical roles in the regulation of PGC differentiation and dedifferentiation. Akt also functions to maintain the pluripotencies of murine and simian ESCs [14].

We investigated the effects of Akt activation on mesoderm induction using an *in vitro* differentiation induction method for murine ESCs on OP9 stromal cells [15]. Activation of Akt signaling induced self-renewing spheres, in which the cells exhibited a metastable differentiation status that was intermediate to those of PGCs and ESCs.

Materials and methods

Cell culturing. The mouse ESCs were maintained as described [14]. Akt-spheres were produced by the protocol used for hematopoietic

* Corresponding authors. Address: Department of Pathology, Medical School, Graduate School of Frontier Biosciences, Osaka University, 2-2 Yamada-oka, Suita, Osaka 565-0871, Japan. Fax: +81 6 6879 3729.
E-mail addresses: tkimura@patho.med.osaka-u.ac.jp (T. Kimura), tnakano@patho.med.osaka-u.ac.jp (T. Nakano).

0006-291X/$ - see front matter © 2010 Elsevier Inc. All rights reserved.
doi:10.1016/j.bbrc.2010.01.005

differentiation induction on OP9 cells [15], in medium with 4OHT (Sigma–Aldrich, St. Louis). Akt-spheres were expanded on the OP9 layer in medium with 4OHT. PD0325901 and CHIR99021 (Stemgent, Cambridge, MA) were used at 1 μM and 3 μM, respectively.

Cell staining. Cell staining was performed by standard method [13]. The primary antibodies used were: anti-Oct-3/4 (BD, Franklin Lakes, NJ); anti-PGC7 (T Nakamura, T.N.); anti-H3K9me2 (Abcam, Cambridge, UK); anti-H3K27me3 (Upstate/Millipore, Billerica, MA); anti-SSEA-1 (Kyowa Medex, Tokyo, Japan); anti-SCP3; anti-β3-tubulin (R&D Systems, Minneapolis, MN), anti-smooth muscle actin (Dako Cytomation, Glostrup, Denmark); and anti-GATA-4 (Santa Cruz Biotechnology, Santa Cruz, CA).

RT-PCR analysis. Total RNA isolation and reverse transcription were performed as described [12]. PCR amplification was carried out with KOD FX (Toyobo, Osaka, Japan). The primer sequences are listed in the Supplementary table.

Transplantation analysis. Akt-sphere cells (60,000 cells) were injected into *W* mutant mouse testis, as described [16]. Two months later, the recipient testes were subjected to histological analysis.

Microarray data analyses. The expression profiles were analyzed using the 3D-Gene Mouse Oligo chip 24 k (Toray Industries, Tokyo, Japan). The fluorescence intensities were detected using the ScanArray Lite Scanner (Perkin–Elmer, Waltham, MA). The PMT levels were adjusted to achieve 0.1–0.5% pixel saturation. Each TIFF image was analyzed using the GenePix Pro ver. 6.0 software (Molecular Devices, Sunnyvale, CA). The data were filtered to remove low-confidence measurements and were globally normalized per array, such that the median of the signal intensity was adjusted to 50 after normalization (accession number GSE18813).

Results

Generation of self-renewing spheres through conditional Akt activation

We used feeder-free mouse E14tg2a ESCs that express myr-Akt-Mer [14], to examine the effect of Akt activation on the *in vitro* differentiation of ESCs to mesoderm. Akt-Mer is composed of a myristoylated, constitutively active form of Akt (myr-Akt) and the ligand-binding domain of a mutant estrogen receptor (Mer). Although the fusion protein is catalytically inactive without the ligand of Mer, 4-hydroxytamoxifen (4OHT), it is rapidly activated by the addition of 4OHT.

The myr-Akt-Mer-expressing ESCs were seeded on OP9 stromal cells with or without 4OHT (Fig. 1A). Whereas mesodermal colonies emerged after 5 days in the absence of 4OHT, mesodermal colonies were scarcely detected in the presence of 4OHT. Although blood cells differentiated in the absence of 4OHT, Akt activation generated floating spheres instead of blood cells (Fig. 1B). The cells composing the spheres showed clear intercellular borders, unlike the ESCs. The spheres were passaged every 4 days on OP9 cells after gentle pipetting or dissociation with trypsin. The spheres

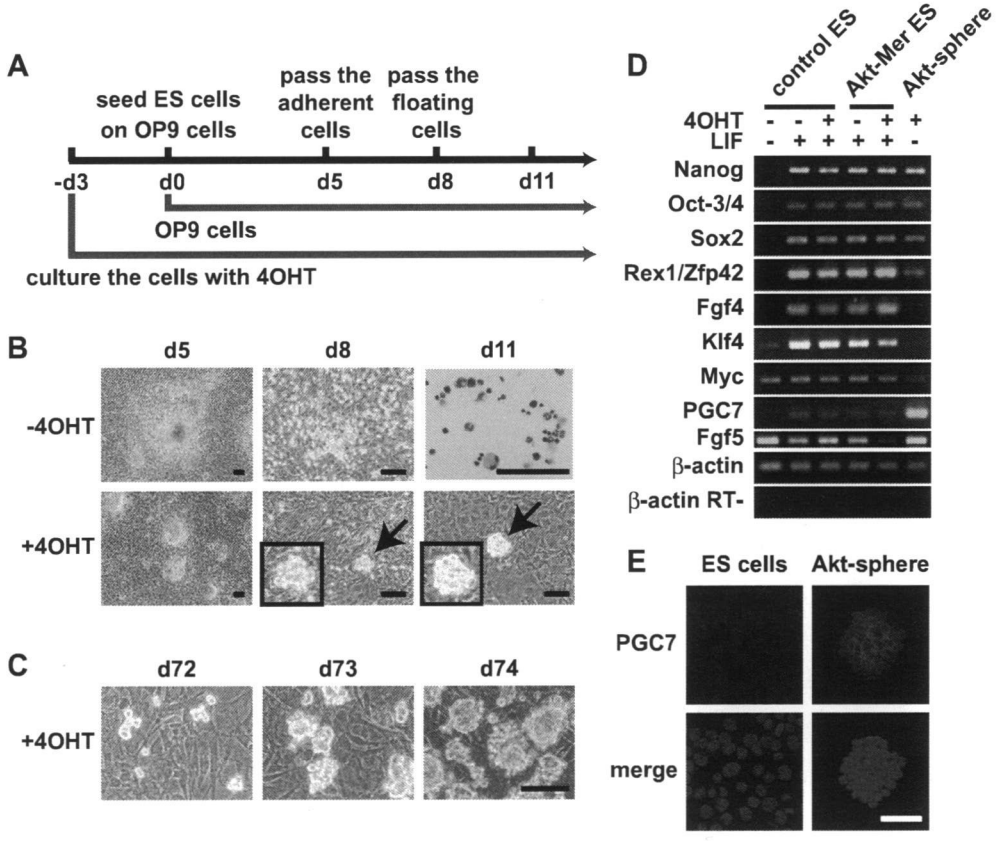

Fig. 1. Production of Akt-spheres. (A) Schematic diagram of Akt-sphere production. The myr-Akt-Mer-expressing ESCs were cultured for 3 days in the presence of 4OHT before transfer to OP9 cells for differentiation induction. On day 5 of induction, the adherent cells were re-seeded onto OP9 cells. Floating cells were re-seeded onto OP9 cells on day 8 of induction. 4OHT treatment was maintained throughout the culture period. (B) Emergence of Akt-spheres. On day 5, mesodermal colonies emerge in the absence of 4OHT but not when 4OHT is present in the medium. Hematopoietic cells appear after day 8 in the absence of 4OHT. Akt activation generates floating spheres (arrows) instead of blood cells. Giemsa staining was performed to identify blood cells on day 11. Scale bars, 100 μm. (C) Expansion of the Akt-spheres. The Akt-spheres were expanded by culturing on OP9 layer with continuous Akt activation. Akt-spheres on day 72 are shown. Scale bar, 100 μm. (D) Expression of pluripotency marker genes. (E) Immunostaining for PGC7. The nuclei are counterstained with DAPI. Scale bar, 50 μm.

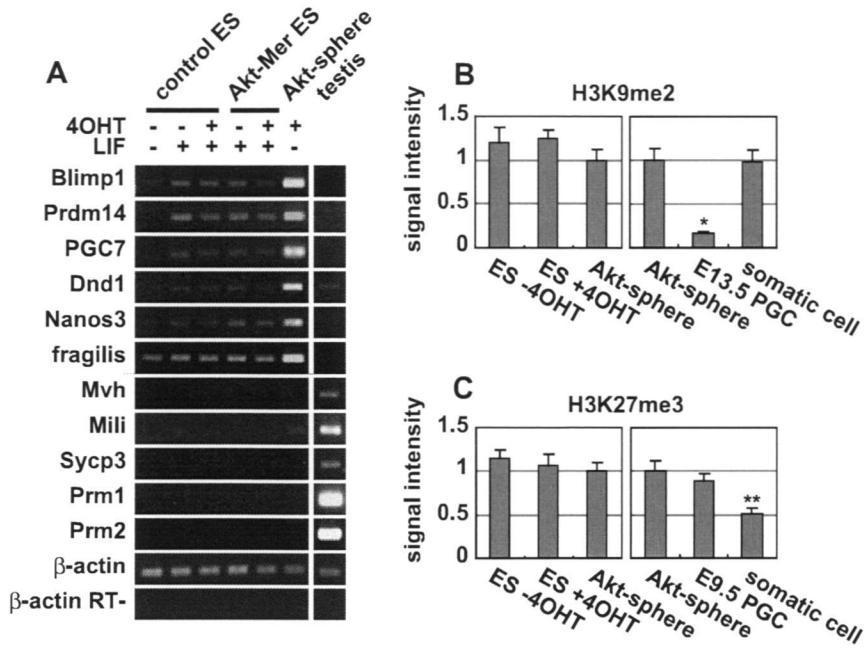

Fig. 2. Expression of germ cell markers and histone modification status. (A) Expression of germ cell marker genes. (B and C) Levels of H3K9me2 and H3K27me3. The cytospun preparations were stained with antibodies against H3K9me2 and H3K27me3 (Fig. S2). The PGCs and somatic cells of E13.5 (B) and E9.5 (C) embryos were used as controls. Signal intensity was measured by LSM5PASCAL confocal laser scanning microscopy. The data shown are mean ± SEM ($n = 10$) and analyzed using the Student's t-test ($^{*}p < 0.001$, $^{**}p < 0.005$).

could be expanded for many generations (Fig. 1C), and a single sphere generated multiple spheres when cultured on an OP9 layer with continuous Akt activation (data not shown). We designated this self-renewing sphere as the 'Akt-sphere'.

Expression of pluripotency genes in Akt-spheres

We examined their expression of mesodermal and pluripotency markers. Consistent with the absence of mesodermal colonies in the 4OHT-treated cultures, the Akt-sphere cells did not express the mesodermal markers (Fig. S1A). In contrast, the Akt-sphere cells expressed the pluripotency markers *Nanog*, *Oct-3/4*, and *Sox2* at the same levels as ESCs (Fig. 1D). Immunostaining showed that Oct-3/4 was expressed in all the sphere cells, as well as in undifferentiated ESCs (Fig. S1B). The expression patterns of the remaining pluripotency genes suggested that the sphere cells more closely resembled PGCs than pluripotent cells, such as ESCs or epiblast cells. First, in the spheres, the expression of *Rex1/Zfp42*, *Fgf4*, and *Klf4* was repressed, whereas the expression of *Fgf5* was increased; these are characteristics of PGCs and epiblasts rather than of ESCs. Second, the *Myc* gene, the expression of which is higher in ESCs and epiblasts than in PGCs, was downregulated in the sphere cells. Third, the expression of *PGC7*, which is dramatically induced in nascent PGCs, was upregulated in the sphere cells. Immunostaining analysis showed that PGC7 was highly expressed in every Akt-sphere cell, mainly in the cytoplasm, as is the case for PGCs (Fig. 1E, S1C). Therefore, the Akt-spheres are composed of a homogeneous cell population that exhibits a PGC-like pluripotency gene expression pattern.

Expression of germ lineage genes and epigenetic status in Akt-spheres

We next investigated the expression of germ cell markers to determine the differentiation stages of the spheres (Fig. 2A). *Blimp1* and *Prdm14* commence expression after E6.25 in PGC precursors [1,3]. These transcriptional regulators of PGC specification were upregulated in the spheres. The expression of *PGC7*, *Dnd1*, *Nanos3*, and *fragilis* starts in the nascent PGC at around E7.0 and is dependent upon Blimp1 and Prdm14. All four genes were expressed at higher levels in the sphere cells than in ESCs. In contrast, *Mvh* and *Mili*, which are induced in PGCs after arrival at the genital ridges, were not upregulated in the sphere cells. Similarly, Akt-sphere cells expressed neither the meiosis marker *Sycp3* nor the spermatogenesis markers *Prm1* and *Prm2*. These results suggest that Akt-sphere cells have the characteristics of PGCs that have not yet arrived at the gonads.

PGCs undergo erasure of H3K9me2 and upregulation of H3K27me3 between E7.75 and E9.5 [5]. The levels of H3K9me2 and H3K27me3 in the Akt-sphere cells were compared with those of undifferentiated ESCs, embryo-derived PGCs, and somatic cells. The H3K9me2 levels were significantly lower in the PGCs than in the ESCs and somatic cells (Fig. 2B, S2A). However, this type of reduction was not observed for the Akt-sphere cells, indicating that genome-wide H3K9 demethylation does not occur in the spheres. In contrast, the levels of H3K27me3 were similar among the Akt-sphere cells, ESCs, and PGCs, whereas the levels of H3K27me3 in the somatic cells were significantly lower (Fig. 2C, S2B). Therefore, the transcriptional cascade specific to nascent PGCs was activated but epigenetic reprogramming was not detected in the Akt-spheres. Taken together, these results demonstrate that Akt-sphere cells possess the characteristics of nascent PGCs at around E7.5, in which the PGC-specification events are initiated but not yet completed.

Transplantation of the Akt-sphere cells into testes

PGCs isolated from embryos after E8.5 and epiblasts at E6.5 can proceed into spermatogenesis after transplantation into the seminiferous tubules of *W* mutant mice [16], which lack spermatogenesis due to *c-Kit* mutations. We injected 60,000 Akt-sphere cells

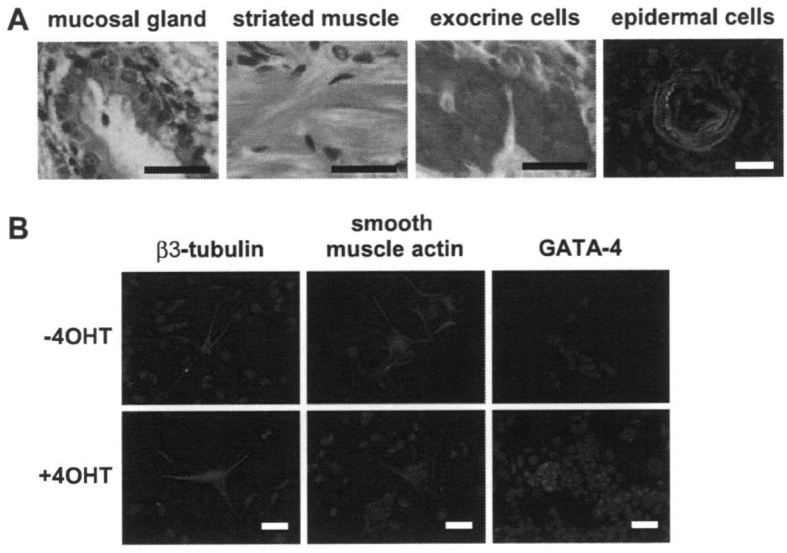

Fig. 3. Differentiation abilities of Akt-sphere cells. (A) Teratoma formation of Akt-sphere cells in the testes of *W* mice. The EGFP-expressing sphere cells (6×10^4) were transplanted into the seminiferous tubules of neonatal *W* mutant mice and analyzed 2 months later. Sections of the recipient testes were analyzed by HE staining or fluorescence microscopy. Scale bars, 30 μm. (B) Multipotential differentiation under feeder-free ESC culture conditions. The Akt-spheres differentiate into β3-tubulin-positive cells, smooth muscle actin-positive cells, and GATA-4-positive cells. The nuclei are counterstained with DAPI. Scale bars, 50 μm.

into testes of neonatal *W* mutant mice, and identified the sphere-derived cells based on EGFP expression. Two months after injection, 9 out of the 10 testes contained EGFP-positive, sphere-derived cells (Fig. S3). Histological analysis revealed that the Akt-sphere cells produced teratomas, which included mucosal glands, striated muscles, exocrine cells, and epidermal cells (Fig. 3A). However, immunostaining with an antibody against SYCP-3 showed a lack of meiotic germ cells (data not shown). Thus, despite the activation of early germ lineage genes, commitment to the germ lineage was incomplete in the spheres.

Multilinege differentiation ability of Akt-sphere cells in original feeder-free ESC culture system

To investigate whether the Akt-spheres contained residual pluripotent ESCs, we transferred the spheres to the feeder-free ESC culture system, which was used to maintain the original ESCs. Even in the presence of LIF, culturing the spheres on gelatin-coated plates induced chaotic differentiation (Fig. 3B). Although 4OHT enhanced cell survival after transfer, differentiation was inevitable and the ESC-like cells did not emerge from the spheres during long-term observation (data not shown). Expression of the pluripotency and germ cell markers was rapidly lost in the sphere-derived cells (Fig. S4). Instead, the spheres differentiated into β3-tubulin-positive ectodermal cells, smooth muscle actin-positive mesodermal cells, and GATA-4-positive endodermal cells, irrespective of 4OHT treatment (Fig. 3B). These results suggest that although Akt-sphere cells possess the ability to differentiate into the three germ layers, they do not maintain the immature state in the original feeder-free culture system.

Reversion of Akt-sphere cells to ESC-like pluripotent cells

Next, we examined whether the Akt-spheres could revert to cells that possessed the characteristics of ESCs. When Akt-spheres were seeded on a mouse embryonic fibroblast (MEF) layer in the presence of 4OHT, the cells still formed floating spheres. However, some of the spheres survived attachment to the MEFs and underwent morphologic changes to ESC-like colonies after the withdrawal of 4OHT (Fig. 4A). A lower number of ESC-like colonies also emerged on the MEFs without transient Akt activation (Fig. S5A). The ESC-like cells could be expanded in response to LIF on MEFs without 4OHT. In addition, the ESC-like cells could be expanded under the feeder-free ESC culture condition, unlike the sphere cells (Fig. 4B), indicating that Akt-sphere cells can be induced to revert to a cell type that is similar to the original ESC by transient culturing on MEFs.

Microarray analysis showed that the ESC-like cells expressed ESC markers, such as *Fgf4*, *Rex1/Zfp42*, *Klf4*, and *Myc*, whereas they showed downregulated expression of the germ cell markers *Prdm14*, *Dnd1*, and *Nanos3* (data not shown). RT-PCR analysis validated these results (Fig. 4D). Hierarchical clustering analysis of the microarray data showed that the global gene expression pattern of the ESC-like cells was more similar to that of the original ESCs than to that of the sphere cells (Fig. 4E, S5B). However, clustering analysis revealed that the gene expression pattern of the ESC-like cells was still intermediate between those of ESCs and sphere cells. Indeed, RT-PCR analysis confirmed that the expression of *Fgf5*, which was downregulated in ESCs, was still upregulated in the ESC-like cells (Fig. 4D).

The "2i" culture system, which contains the ERK cascade inhibitor PD0325901 or PD184352 and the GSK3 inhibitor CHIR99021, maintains ESCs in basal state pluripotency [17] and converts epiblast stem cells (EpiSCs) to the ESC state [18]. The Akt-spheres were transferred to feeder-free dishes in medium supplemented with PD0325901 and CHIR99021. The 2i condition generated ESC-like colonies after 7 days of culture, irrespective of 4OHT treatment (Fig. 4C, S5C). In addition, ESC markers were expressed and germ cell markers were suppressed in the ESC-like cells (Fig. 4D). Therefore, culturing the spheres on MEFs or under the 2i condition induces reversion to the ESC-like state.

Discussion

Blimp1 and Prdm14 repress the somatic program, activate PGC-specific genes, and re-activate pluripotency genes, in lineage-restricted PGC precursors from E6.75 to E7.0 [4]. Akt activation inhibited mesodermal differentiation from ESCs before the emergence of

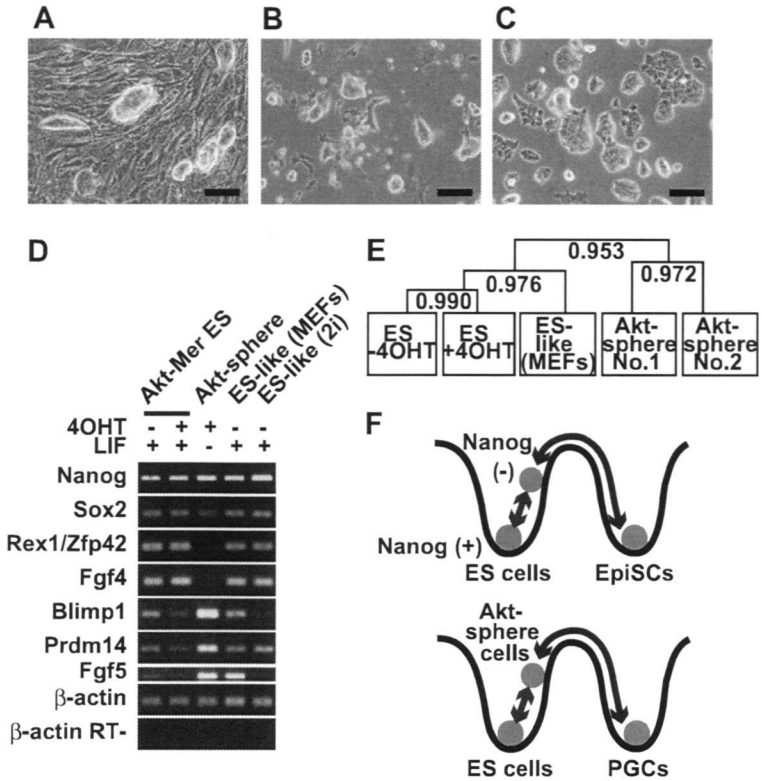

Fig. 4. Derivation of ESC-like cells from Akt-spheres. (A and B) Derivation of ESC-like cells by culturing Akt-spheres on MEFs. Akt-spheres were seeded onto MEFs and cultured in the presence of 4OHT and LIF for 5 days. These cells form ESC-like colonies when transferred to MEFs in the absence of 4OHT (A). After reversion to ESC-like cells, these cells can be expanded without MEFs (B). Scale bars, 100 μm. (C) Derivation of ESC-like cells under the 2i culture condition. Scale bar, 100 μm. (D) Expression of pluripotency and germ cell markers in the ESC-like cells. (E) Whole genome cluster analysis of transcripts. The RNA species from the Akt-Mer ESCs treated with or without 4OHT, the ESC-like cells that emerged on the MEFs, and the sphere cells that were induced from two independent Akt-Mer ESC lines were subjected to microarray analysis. Similarity of global gene expression patterns was measured by Pearson correlation of log-transformed expression values after global normalization. The correlation coefficients are indicated. (F) Model summarizing the metastable pluripotency state of the Akt-sphere cells. The differentiation state at the bottom of the "bowl", which is thermodynamically more stable than that at the "hilltop" in this model, is stabilized by intrinsic and external factors [28]. One cell state can be "lifted-up" and "moved" to another cell state by appropriate stimuli. The murine ESC-like state is stabilized by the LIF, while bFGF/activin stabilizes the EpiSC-like state (upper panel). A metastable equilibrium exists between the ESC subpopulation (red arrows). The ESC-like and the EpiSC-like states are inter-convertible (blue arrows). Similarly, the pluripotent cells give rise to PGCs, which can be reverted to the ESC-like state by bFGF, LIF, and SCF (bottom panel, blue arrows). The Akt-sphere cells are induced from ESCs by the mesoderm-induction signals from OP9 cells and Akt activation, whereas the sphere cells are reverted to the ESC-like state by culturing on MEFs or under the 2i culture condition in response to LIF (red arrows). (For interpretation of references to color in this figure legend, the reader is referred to the web version of this article.)

Akt-spheres, and mesodermal genes were not induced in the sphere cells. Considering that PGCs are specified under the influences of mesoderm-induction signals, it is likely that blockade of mesodermal fate by Akt activation is a prerequisite for the PGC-like state under the mesoderm-inducing culture condition. In addition to the repressed somatic gene expression program, Akt-sphere cells activated PGC-specific genes and expressed pluripotency genes. However, downregulation of H3K9me2, which occurred from E7.75 to E9.5 [5] in PGCs did not take place in the spheres. Therefore, Akt-spheres acquire the characteristics of nascent PGCs at E6.75–E7.75.

The Akt-spheres failed to undergo spermatogenesis in the testes of *W* mice. It has been reported that E6.5 epiblast cells that contain PGC precursors differentiate into round spermatids in this transplantation assay, albeit at a low frequency [16]. However, germ line specification appears to be incomplete in the Akt-spheres. Given that Akt activation promotes the dedifferentiation of PGCs [12,13], some of the processes required for germ cell specification appear to be defective in the spheres.

Akt-spheres differentiated into the three germ layers both in the recipient testes and in feeder-free ESC cultures, demonstrating that the spheres possess pluripotency. The pluripotency state of the spheres was somewhat different from that of the original ESCs, since the spheres were completely differentiated after transfer to feeder-free ESC cultures, even in the presence of LIF. The expression pattern of the pluripotency-related genes in the sphere cells was similar to those of the epiblast cells and PGCs (Fig. 1D). These results suggest that Akt-spheres are in a pluripotency state that is intermediate between those of ESCs and PGCs.

In contrast to the results obtained in feeder-free cultures, culturing on an MEF layer or under the 2i condition resulted in the sphere cells being reverted to ESC-like cells. These results suggest that ESCs and Akt-sphere cells are in 'metastable' equilibrium. The term 'metastability' was originally used to describe a spontaneous interconversion between ESC subpopulations, such as transient oscillation between Nanog-positive and Nanog-negative cell populations (Fig. 4F, upper panel) [19,20]. According to these models, stem cells can fluctuate between different epigenetic and phenotypic states while undergoing self-renewal in culture. This concept has been extended to describe an interconversion between two differentiation states that is induced by the appropriate culture conditions or by the introduction of specific genes [18,21]. ESCs give rise to EpiSC-like cells upon transfer to EpiSC culture conditions, whereas EpiSCs are converted to ESC-like cells by culturing under

the 2i condition and/or the introduction of Klf4 [18,21]. Furthermore, epiblast cells isolated from embryos can be reprogrammed to the ESC-like state on MEFs in response to LIF, as is the case for Akt-sphere cells [22]. In this regard, PGCs may also be in a metastable state, since PGCs are derived from epiblast cells and converted to EG cells by treatment with growth factors (Fig. 4F, bottom panel) [6,7].

In contrast, the pluripotency state of Akt-sphere cells is intermediate between those of ESCs and PGCs, as discussed above. Since it has been postulated that epigenetic reprogramming events occurring during PGC differentiation serve as an 'epigenetic barrier' to discriminate between pluripotent cells and PGCs [23], incomplete reprogramming of the sphere cells may cause reversion to the ESC-like state. Similarly, it has been recently reported that PGC-like cells spontaneously emerge from EpiSCs and can be reverted to EpiSCs under the EpiSC culture conditions [24]. The EpiSC-derived PGC-like cells appear to have differentiated to a more advanced stage than the Akt-sphere cells, as downregulation of H3K9me2 was observed in the EpiSC-derived cells. Thus, the culture conditions induced distinct PGC-like metastable differentiation states, which may be valuable in understanding metastability between pluripotent cells and PGCs.

The PI3K/Akt and JAK/STAT3 signaling pathways, both of which are activated downstream of LIF, are central to the maintenance of murine ESC pluripotency [25]. Activation of Akt or STAT3 sufficiently supports the mouse ESC pluripotency in the absence of LIF [14,26]. In contrast to the situation for ESCs, LIF/JAK/STAT3 signaling is dispensable for EpiSC self-renewal, which, instead, can be maintained with bFGF and activin [25]. Primate ESCs share several characteristics with EpiSCs, such as morphology, gene expression profiles, epigenetic status, and responsiveness to bFGF/activin. Activated Akt supports the pluripotency of cynomolgus monkey ESCs without bFGF/activin [14]. Since bFGF is a potent activator of PI3K/Akt signaling, the self-renewal of primate ESCs may be promoted by PI3K/Akt signaling downstream of bFGF. In this regard, it is noteworthy that Akt signaling is activated in PGCs by bFGF, which is essential for EG cell derivation, and Akt activation replaces to some extent the effects of bFGF on EG cell derivation [13]. In addition, this study reveals that Akt activation is required for the induction and expansion of Akt-sphere cells. Therefore, PI3K/Akt signaling supports the pluripotency of various cell types.

The production of "functional" gametes from ESCs *in vitro* still remains controversial. Recently, it has been reported that epiblasts isolated from mouse embryos differentiate into PGC-like cells *in vitro*, and that these cells differentiate in the *W* mice testes into spermatids that support the generation of live offspring [27]. Although our PGC-like cells failed to produce gametes in the recipient testes, the derivation of functional PGCs would be the first step in reconstituting germ cell differentiation from ESCs *in vitro*.

Acknowledgments

The authors thank Drs. Chuma and Nakatsuji for SYCP-3 antibody, Drs. Sudo and Akiyama (Toray New Frontiers Research Laboratories) for microarray analysis, and Dr. Morii for advices. This work was supported in part by grants from the Japan Society for the Promotion of Science, the Ministry of Education, Culture, Sports, Science and Technology of Japan, and the Sankyo Foundation of Life Science.

Appendix A. Supplementary data

Supplementary data associated with this article can be found, in the online version, at doi:10.1016/j.bbrc.2010.01.005.

References

[1] Y. Ohinata, B. Payer, D. O'Carroll, et al., Blimp1 is a critical determinant of the germ cell lineage in mice, Nature 436 (2005) 207–213.
[2] S.D. Vincent, N.R. Dunn, R. Sciammas, et al., The zinc finger transcriptional repressor Blimp1/Prdm1 is dispensable for early axis formation but is required for specification of primordial germ cells in the mouse, Development 132 (2005) 1315–1325.
[3] M. Yamaji, Y. Seki, K. Kurimoto, et al., Critical function of Prdm14 for the establishment of the germ cell lineage in mice, Nat. Genet. 40 (2008) 1016–1022.
[4] K. Kurimoto, Y. Yabuta, Y. Ohinata, et al., Complex genome-wide transcription dynamics orchestrated by Blimp1 for the specification of the germ cell lineage in mice, Genes Dev. 22 (2008) 1617–1635.
[5] Y. Seki, M. Yamaji, Y. Yabuta, et al., Cellular dynamics associated with the genome-wide epigenetic reprogramming in migrating primordial germ cells in mice, Development 134 (2007) 2627–2638.
[6] Y. Matsui, K. Zsebo, B.L. Hogan, Derivation of pluripotential embryonic stem cells from murine primordial germ cells in culture, Cell 70 (1992) 841–847.
[7] J.L. Resnick, L.S. Bixler, L. Cheng, et al., Long-term proliferation of mouse primordial germ cells in culture, Nature 359 (1992) 550–551.
[8] C.L. Stewart, I. Gadi, H. Bhatt, Stem cells from primordial germ cells can reenter the germ line, Dev. Biol. 161 (1994) 626–628.
[9] G. Durcova-Hills, F. Tang, G. Doody, et al., Reprogramming primordial germ cells into pluripotent stem cells, PLoS One 3 (2008) e3531.
[10] L.C. Stevens, Origin of testicular teratomas from primordial germ cells in mice, J. Natl. Cancer Inst. 38 (1967) 549–552.
[11] B. Stiles, M. Groszer, S. Wang, et al., PTENless means more, Dev. Biol. 273 (2004) 175–184.
[12] T. Kimura, A. Suzuki, Y. Fujita, et al., Conditional loss of PTEN leads to testicular teratoma and enhances embryonic germ cell production, Development 130 (2003) 1691–1700.
[13] T. Kimura, M. Tomooka, N. Yamano, et al., AKT signaling promotes derivation of embryonic germ cells from primordial germ cells, Development 135 (2008) 869–879.
[14] S. Watanabe, H. Umehara, K. Murayama, et al., Activation of Akt signaling is sufficient to maintain pluripotency in mouse and primate embryonic stem cells, Oncogene 25 (2006) 2697–2707.
[15] T. Nakano, H. Kodama, T. Honjo, Generation of lymphohematopoietic cells from embryonic stem cells in culture, Science 265 (1994) 1098–1101.
[16] S. Chuma, M. Kanatsu-Shinohara, K. Inoue, et al., Spermatogenesis from epiblast and primordial germ cells following transplantation into postnatal mouse testis, Development 132 (2005) 117–122.
[17] Q.L. Ying, J. Wray, J. Nichols, et al., The ground state of embryonic stem cell self-renewal, Nature 453 (2008) 519–523.
[18] J. Hanna, S. Markoulaki, M. Mitalipova, et al., Metastable pluripotent states in NOD-mouse-derived ESCs, Cell Stem Cell 4 (2009) 513–524.
[19] K. Hayashi, S.M. Lopes, F. Tang, et al., Dynamic equilibrium and heterogeneity of mouse pluripotent stem cells with distinct functional and epigenetic states, Cell Stem Cell 3 (2008) 391–401.
[20] I. Chambers, J. Silva, D. Colby, et al., Nanog safeguards pluripotency and mediates germ line development, Nature 450 (2007) 1230–1234.
[21] G. Guo, J. Yang, J. Nichols, et al., Klf4 reverts developmentally programmed restriction of ground state pluripotency, Development 136 (2009) 1063–1069.
[22] S. Bao, F. Tang, X. Li, et al., Epigenetic reversion of post-implantation epiblast to pluripotent embryonic stem cells, Nature 461 (2009) 1292–1295.
[23] K. Hayashi, M.A. Surani, Resetting the epigenome beyond pluripotency in the germline, Cell Stem Cell 4 (2009) 493–498.
[24] K. Hayashi, M.A. Surani, Self-renewing epiblast stem cells exhibit continual delineation of germ cells with epigenetic reprogramming in vitro, Development 136 (2009) 3549–3556.
[25] J. Nichols, A. Smith, Naive and primed pluripotent states, Cell Stem Cell 4 (2009) 487–492.
[26] T. Matsuda, T. Nakamura, K. Nakao, et al., STAT3 activation is sufficient to maintain an undifferentiated state of mouse embryonic stem cells, EMBO J. 18 (1999) 4261–4269.
[27] Y. Ohinata, H. Ohta, M. Shigeta, et al., A signaling principle for the specification of the germ cell lineage in mice, Cell 137 (2009) 571–584.
[28] T. Enver, M. Pera, C. Peterson, et al., Stem cell states, fates, and the rules of attraction, Cell Stem Cell 4 (2009) 387–397.

TISSUE ENGINEERING: Part C
Volume 00, Number 00, 2009

DOI: 10.1089/ten.tec.2009.0277

Methods Article

Validation System of Tissue-Engineered Epithelial Cell Sheets for Corneal Regenerative Medicine

Ryuhei Hayashi, Ph.D.,[1] Masayuki Yamato, Ph.D.,[2] Hiroshi Takayanagi, M.Sc.,[1] Yoshinori Oie, M.D.,[1] Akira Kubota, Ph.D., M.D.,[1] Yuichi Hori, Ph.D., M.D.,[3] Teruo Okano, Ph.D.,[2] and Kohji Nishida, M.D., Ph.D.[1]

Recently, regenerative therapy with tissue-engineered epithelial cell sheets has been performed for treating ocular surface disease. It would be required to develop the validation method for these cell sheets to standardize and spread the regenerative therapy. In the present study, we developed a validation system for cultivated epithelial cell sheets. Human limbal epithelial cells and human oral mucosal epithelial cells were cultured with 3T3 feeder layer cells on temperature-responsive culture inserts for three different culture periods, and subjected to cell sheet harvest and validation. Epithelial cells cultured for a short period were not successfully harvested as intact contiguous cell sheets. On the other hand, total cell number and viability of epithelial cell sheets harvested after prolonged culture period decreased. Further, these cells also lost epithelial barrier function. These results showed the potential effectiveness of the proposed validation system that can evaluate fabricated cell sheets before transplantation.

Introduction

CORNEAL EPITHELIAL STEM CELLS reside in the basal layer of the limbus, the transitional zone between the cornea and the bulbar conjunctiva.[1] These cells govern renewal of the corneal epithelium by generating progeny (transient amplifying cells, which are the cells committed to epithelial differentiation) with limited renewal capabilities that migrate from the limbus into the basal layer of the cornea.[2,3] If corneal epithelial stem cells are completely absent owing to limbal disorder from severe trauma or eye diseases, then the sources of corneal epithelial cells have been exhausted, the peripheral conjunctival epithelium invades inwardly, and the corneal surface becomes enveloped by vascularized conjunctival scar tissue, resulting in corneal opacification that leads to severe visual impairment. Such pathological characteristics are considered to represent limbal stem-cell deficiencies.[4,5]

For patients with unilateral or bilateral limbal stem-cell deficiencies, limbal allograft transplantation can be performed,[6] but it requires long-term immunosuppression that involves high risks of serious eye and systemic complications, including infection and liver and kidney dysfunction.[7] In patients with the Stevens–Johnson syndrome or ocular pemphigoid, graft failure is common, even with immunosuppression, owing to serious preoperative conditions such as persistent inflammation of the ocular surface, abnormal epithelial differentiation of the ocular surface, severe dry eyes, and lid-related abnormalities.[7–9] Therefore, we have performed a regenerative therapy for such patients with severe corneal epithelial disease by transplantation of functional tissue-engineered epithelial cell sheets fabricated on temperature-responsive culture surfaces.[10,11] By utilizing temperature-responsive culture surfaces, noninvasive cell sheet harvest is reproducibly achieved, since the surfaces reversibly change the hydrophobic/hydrophilic property depending on temperature across 32°C. Only by reducing temperature below 32°C, all the cultured cells are harvested as a single contiguous cell sheet without need for proteolytic enzymes. Cell sources are patient's own healthy limbus and oral mucosa for unilateral and bilateral disease cases, respectively.

Recently, several groups have also reported similar epithelial cell transplantation to treat ocular surface disease.[12–14] These reports, including ours, showed that epithelial cell sheet transplantation was effective in the treatment of severe ocular surface diseases. However, there are no detailed descriptions regarding the cell sheet quality that would be assessed by each researcher. Moreover, it is now the next step to develop the corneal epithelial regenerative therapy from clinical trials into a standard medical therapy, and for this it is important to precisely validate the final products before transplantation to determine whether they can be used or not. Here we would like to propose a validation system

[1]Department of Ophthalmology, Tohoku University Graduate School of Medicine, Sendai, Japan.
[2]Institute of Advanced Biomedical Engineering and Science, Tokyo Women's Medical University, Tokyo, Japan.
[3]Department of Ophthalmology, Osaka University School of Medicine, Suita, Japan.

composed of the following evaluation items: (1) cell morphology, (2) cell sheet recovery, (3) total cell number, (4) cell viability, (5) epithelial cell purity, (6) degree of stratification, (7) existence of epithelial stem/progenitor cells, (8) cell differentiation, and (9) existence of barrier function. In the present study, we evaluated transplantable human epithelial cell sheets with different culture periods to confirm the usefulness of the proposed validation system.

Materials and Methods

Epithelial cell culture

Human limbal tissues were isolated from corneoscleral rims isolated from cadaveric donor corneas (Northwest Lions Eye Bank, Seattle, WA) using scissors ($n=4$). Human oral mucosal tissue (~3×3 mm specimen) was surgically excised from a healthy volunteer's interior buccal mucosa under local anesthesia with xylocaine ($n=3$). Each tissue was washed with Dulbecco's phosphate-buffered saline containing antibiotics and antimycotics, and incubated with dispase II at 37°C for 1 h. Separated epithelial layer was treated with trypsin–ethylenediaminetetraacetic acid (EDTA) solution (Invitrogen, Carlsbad, NM), and resuspended cells were plated on temperature-responsive culture inserts (CellSeed, Tokyo, Japan) at an initial cell density of 1.5×10^5 cells (limbal epithelial cells) or 2.0×10^5 cells (oral mucosal epithelial cells)/23-mm insert with mitomycin C–treated NIH/3T3 cells separated by cell culture inserts in the keratinocyte culture medium (KCM) (Dulbecco's modified Eagle's medium [DMEM]/F12 [3:1] supplemented with 10% fetal bovine serum [Japan Bio Serum, Hiroshima, Japan], 0.5% Insulin–Transferrin–Selenium [ITS; Invitrogen], 10 μM isoproterenol [Kowa, Tokyo, Japan], 2.0×10^{-9} M triiodothyronine [MP Biomedicals, Aurora, OH], 0.4 μg/mL hydrocortisone succinate [Wako, Osaka, Japan], and 10 ng/mL EGF [R&D Systems, Minneapolis, MN]).[10] All the procedures for the validation system were performed within the day when the cell culture was terminated (Fig. 1).

Phase contrast microscopy

The cultured epithelial cells were observed under a phase contrast microscope, and microphotographs were taken at 50-fold and 100-fold magnification (Axiovert 40; Carl Zeiss, Jena, Germany) to examine cell morphological aberration and deficits.

Sheet recovery test

After being examined by phase contrast microscopy, the cultured epithelial cells were subjected to incubation at 20°C for 30 min in an incubator of 5% CO_2. Then, a donut-shaped support membrane (18 mm in outer diameter and 10 mm in inner diameter; polyvinylidene difluoride; Millipore, Bedford, MA) was placed on the epithelial cells. Finally, the cells were challenged to cell sheet harvest together with support membranes. The harvested epithelial cell sheets were bisected. One of the bisected cell sheets was subjected to counting of total cell number and flow cytometric analyses, and the other was subjected to histological analyses (Fig. 1).

Total cell number

Bisected cell sheets were incubated with 0.25% trypsin–EDTA at 37°C for 10 min to obtain single-cell suspension. The enzymatic reaction was stopped by adding DMEM containing 5% fetal bovine serum. After centrifugation, the cells were resuspended in DMEM, and the cell number was counted with a Burker–Turk hemocytometer.

Cell viability

Cell viability was evaluated with dye exclusion test. An aliquot of cell suspension was incubated in DMEM with 7-aminoactinomycin D (7′AAD; BD Biosciences, San Diego, CA) staining at room temperature for 10 min, and subjected to flow cytometer (FACS Calibur; BD Biosciences).

Epithelial cell purity

An aliquot of cell suspension after trypsin–EDTA treatment was centrifuged, fixed, and permeabilized with Cytofix/Cytoperm kit (BD Biosciences) according to the manufacturer's protocols. Then, the cell suspension was split into two tubes, and reacted with either fluorescein isothiocyanate–conjugated antipancytokeratin immunoglobulin G2a (IgG2a) antibody (clone PAn1-8; Progen, Heidelberg, Germany) or fluorescein isothiocyanate–conjugated mouse control IgG2a antibody (Santa Cruz Biotechnology, Santa Cruz, CA) at room temperature for 60 min. After being washed with phosphate-buffered saline twice, the cells were stained with 7′AAD for the nuclear staining and examined by flow cytometry.

Hematoxylin and eosin staining

Hematoxylin and eosin (HE) staining was performed on the other bisected cell sheets to examine the degree of stratification of epithelial cells in the harvested cell sheets. The bisected cultured epithelial cell sheets were embedded in Tissue-Tek® O.C.T™ compound (Sakura Seiki, Tokyo, Japan), and processed into 10-μm-thick frozen sections. After being dried for 1 h at room temperature, tissues were washed three times with Tris-buffered saline (TBS; Takara Bio, Shiga, Japan), and fixed with 10% formaldehyde at room temperature for 30 min. The sections were washed with TBS twice and then stained with HE. Microphotographs were taken with a light microscope (Carl Zeiss, Jena, Germany), and the degree of stratification was examined.

Immunofluorescence analyses

Frozen sections were incubated with TBS containing 5% donkey serum and 0.3% Triton X-100 for 1 h to block nonspecific reactions. Sections were then incubated with anti-p63 antibody (4A4; Santa Cruz Biotechnology), anti-cytokeratin 3/2p antibody (AE5; Progen), anti-ZO-1 antibody (1A12; Zymed, South San Francisco, CA), or anti-MUC16 antibody (Ov185; AbCam, Cambridge, United Kingdom) at room temperature for 1.5 h. The slides were washed with TBS twice and then incubated with Alexa Flour 488–conjugated anti-mouse IgG antibody (Molecular Probes, Eugene, OR) at room temperature for 1 h. After being washed with TBS twice, the sections were counterstained with Hoechst 33342 (Molecular Probes) for 10 min and mounted with Perma-Fluor (Beckman Coulter, Miami, FL). The slides were observed using fluorescent microscopy (Axiovert 40; Carl Zeiss).

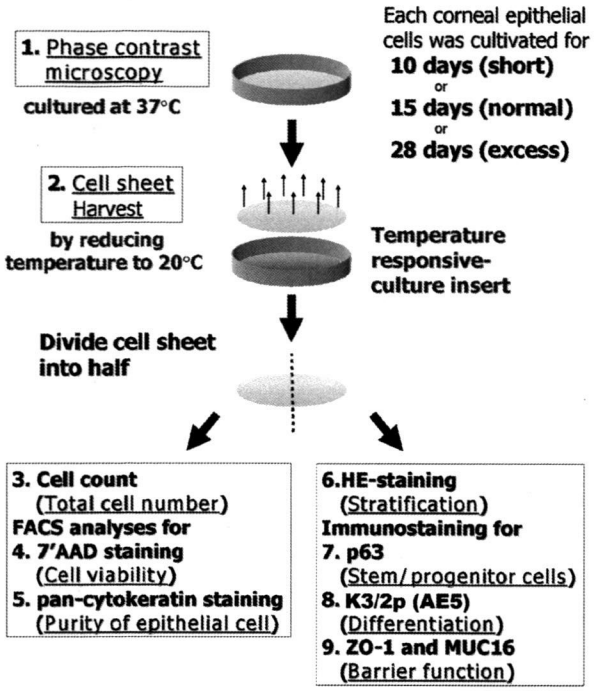

FIG. 1. Validation system. Human limbal epithelial cells were cultured on temperature-responsive cell inserts for 10, 15, and 28 days. Cell morphological examination was performed by phase contrast microscopy, and then cultured epithelial cells were harvested by reducing temperature to 20°C. Harvested cell sheets were divided into two halves. One was used for cell counting and flow cytometric analyses, and the other for hematoxylin and eosin (HE) staining and immunostaining for p63, K3/2p, ZO-1, and MUC16, to validate the quality of cell sheets. All of these procedures were performed within the day when cell culture was terminated.

Results

Phase contrast microscopy revealed that human epithelial cells obtained from a piece of limbal tissue proliferated and stratified on day 15 under the present culture condition. These cells showed tight and dense packing on culture inserts as well as cobble stone–like cell morphology, which is specific to stratified squamous epithelial cells (Fig. 2). In contrast, cell density was still low on day 10. Some defects and denucleated cells were found on day 28. Coinciding with the phase contrast microscopic results, all the epithelial cells on the temperature-responsive culture insert were successfully harvested as a single contiguous cell sheet on day 15. No defects or damage was observed in the harvested cell sheets. Similarly, all the epithelial cell sheets cultured for 28 days were also harvested as cell sheets, but the harvested cell sheets were more fragile than those cultured for 15 days and partially broken. These epithelial cells cultured for 10 days were not harvested as cell sheets, implying insufficient cell packing and stratification. Averages of total cell number in corneal epithelial cell sheets harvested on days 15 and 28 were 11.0×10^5 and 5.1×10^5 cells, respectively. Dye exclusion tests with flow cytometric analysis after membrane-impermeable 7'AAD staining revealed that cell viability was satisfying on day 15 (93.2%), but significantly decreased (64.1%) after prolonged culture of 28 days (Fig. 3). However, epithelial cell purity of the harvested cell sheets determined by flow cytometric analysis after pancytokeratin staining was essentially the same in both of the cell sheets (>95%) (Fig. 3).

Stratification of epithelial cells in harvested sheets was evaluated on HE-stained sections (Fig. 4). Epithelial cell sheets harvested on day 15 comprised of four to eight layers of epithelial cells, and each stratified layer resembled basal, wing, and superficial squamous epithelial cells in morphology as observed in native corneal epithelia. However, fragile cell sheets harvested on day 28 comprised of only one to three epithelial cell layers. p63, a marker of epithelial stem/progenitor cells,[15,16] was expressed in the basal cell layers of both the harvested cell sheets (Fig. 4). Cells positively reacted with anti-cytokeratin 3/2p (corneal and oral mucosal differentiated epithelial cell markers)[1] monoclonal antibody (clone AE5) detected predominantly in both cell sheets, but it was faint in the basal cell layer of cell sheets harvested on day 15. Two essential molecules for epithelial barrier function of ZO-1 in tight junctions[17] as well as a membrane-associated mucin, MUC16, specific to ocular surfaces[18] were expressed continuously throughout superficial cells in cell sheets harvested on day 15. On the other hand, ZO-1 and MUC16 were faintly and discontinuously expressed in the superficial cells in cell sheets harvested on day 28. These results are summarized in Table 1.

In our protocol for corneal regenerative therapy, patients' own oral mucosal tissues are used as an epithelial cell source in bilateral cases.[19,20] Therefore, we performed the present validation for not only human corneal epithelial cell sheets (Fig. 5; $n=3$), but also human oral mucosal epithelial cell sheets ($n=3$) cultured for appropriate periods of 13–16 days determined by the phase contrast microscopic observation. The result showed that there were no remarkable differences between oral mucosal and corneal epithelial cell sheets in each examination (Table 2). Each examination was performed stably in every cell sheet validation.

Discussion

In this study, we performed the validation of the epithelial cell sheet based on the following evaluation items: (1) cell morphology, (2) cell sheet recovery, (3) total cell number, (4) cell viability, (5) epithelial cell purity, (6) degree of stratification, (7) existence of epithelial stem/progenitor cells, (8) differentiation state, and (9) existence of barrier function. Obtained results show that this validation system successfully detected differences in the quality of corneal epithelial cells cultured for different periods. With the same methods, we reproducibly performed the validations of human corneal and oral mucosal epithelial cell sheets cultured for appropriate periods.

In this validation system, cell sheet recovery test could be the most important, because cell sheets are fabricated on temperature-responsive culture surfaces and have no carriers for transplantation such as amniotic membrane or type I collagen sheets. In the present study, it was shown that cell sheets were too fragile for harvest and transplantation after 10-day culture. This might be caused by insufficiency of cell number, cell stratification, intercellular adhesion, and deposition of extracellular matrix. This finding also indicated that

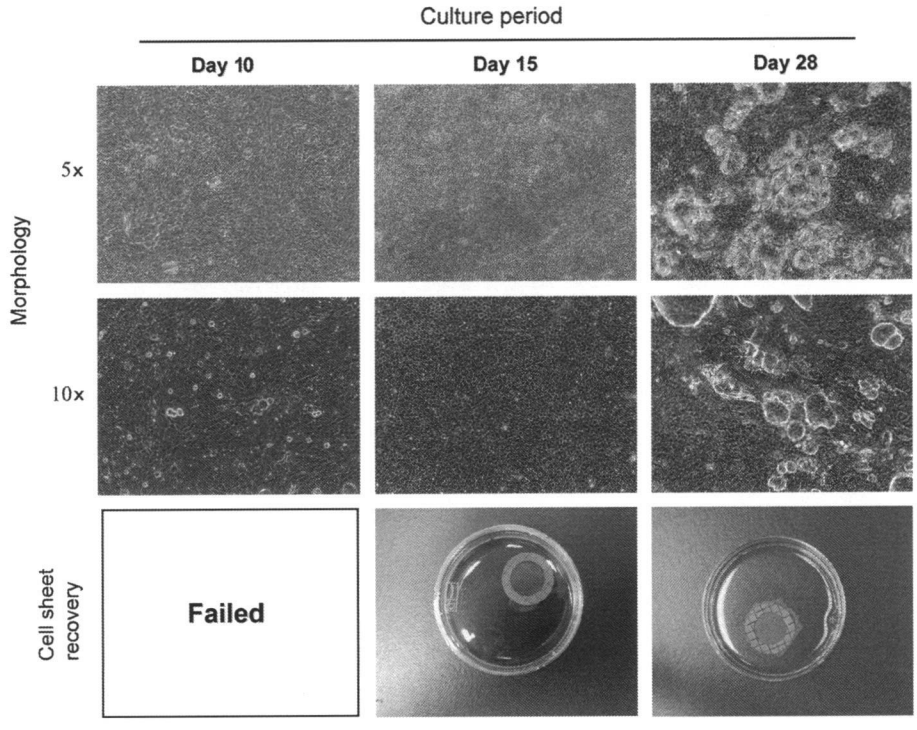

FIG. 2. Cell morphology and cell sheet harvest. Cell morphology was examined by phase contrast microscopy. Harvested cell sheets with supporter membranes were transferred into culture medium in 60-mm dishes. Cells cultured for 10 days were not successfully harvested from temperature-responsive inserts (denoted as "Failed"). Color images available online at www.liebertonline.com/ten.

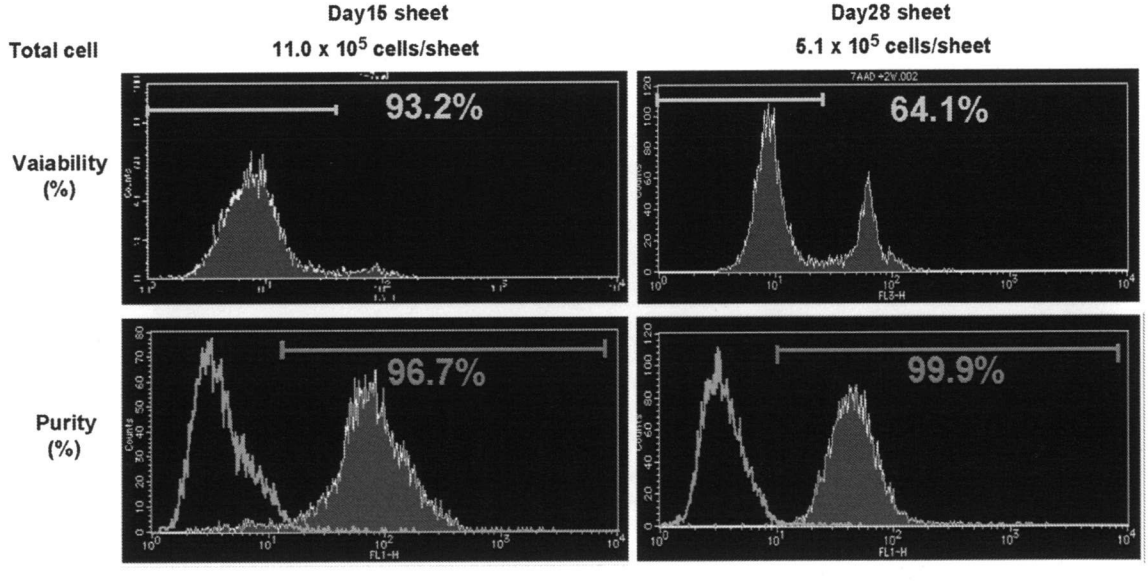

FIG. 3. Flow cytometric analyses. Harvested cell sheets were incubated with trypsin–ethylenediaminetetraacetic acid to obtain single-cell suspension. Resuspended cells were analyzed in cell viability and epithelial cell purity by staining with 7-aminoactinomycin D (7′AAD) and antipancytokeratin antibody, respectively. Color images available online at www .liebertonline.com/ten.

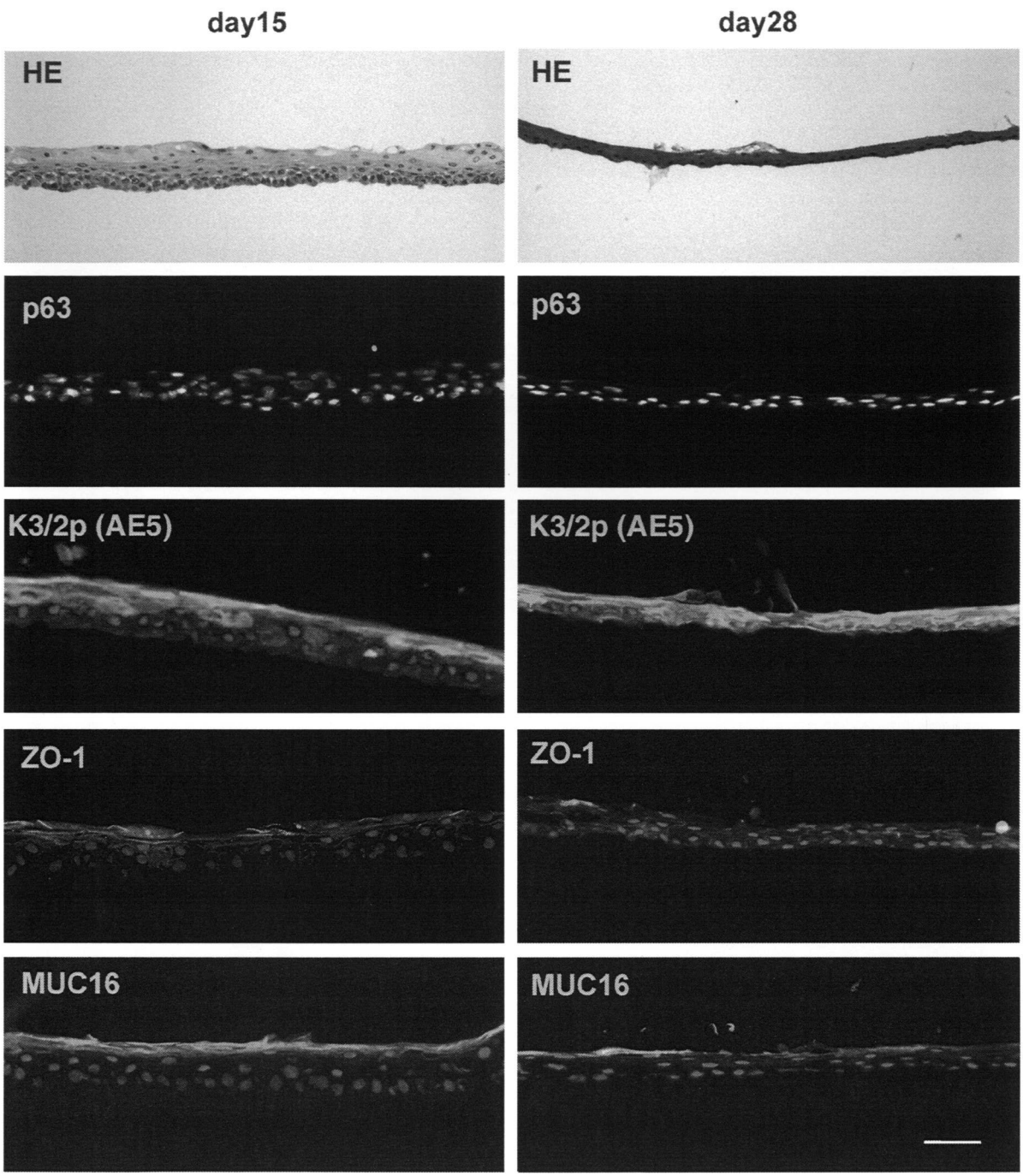

FIG. 4. Histological analyses. Frozen sections of harvested cell sheets were subjected to HE staining and immunofluorescence with anti-p63, anti-K3/2p, anti-ZO-1, or anti-MUC16 antibodies.

TABLE 1. SUMMARY OF VALIDATION OF HUMAN CORNEAL EPITHELIAL CELLS CULTURED FOR DIFFERENT PERIODS

	Phase contrast	*Detachment test*	*Cell ($\times 10^5$)*	*Viability (%)*	*Purity (%)*	*Stratification (HE)*	*p63*	*K3/2p*	*Muc16 ZO-1*
Day 10	Low density	Impossible	—	—	—	—	—	—	—
Day 15	Normal	Possible	11.0	93.2	96.8	Normal 4–8 layers	Posi	Posi	Posi
Day 28	Defects	Partially broken	5.1	64.1	99.9	Thin 2–3 layers	Posi	Posi	Faint

HE, hematoxylin and eosin; Posi, positive.

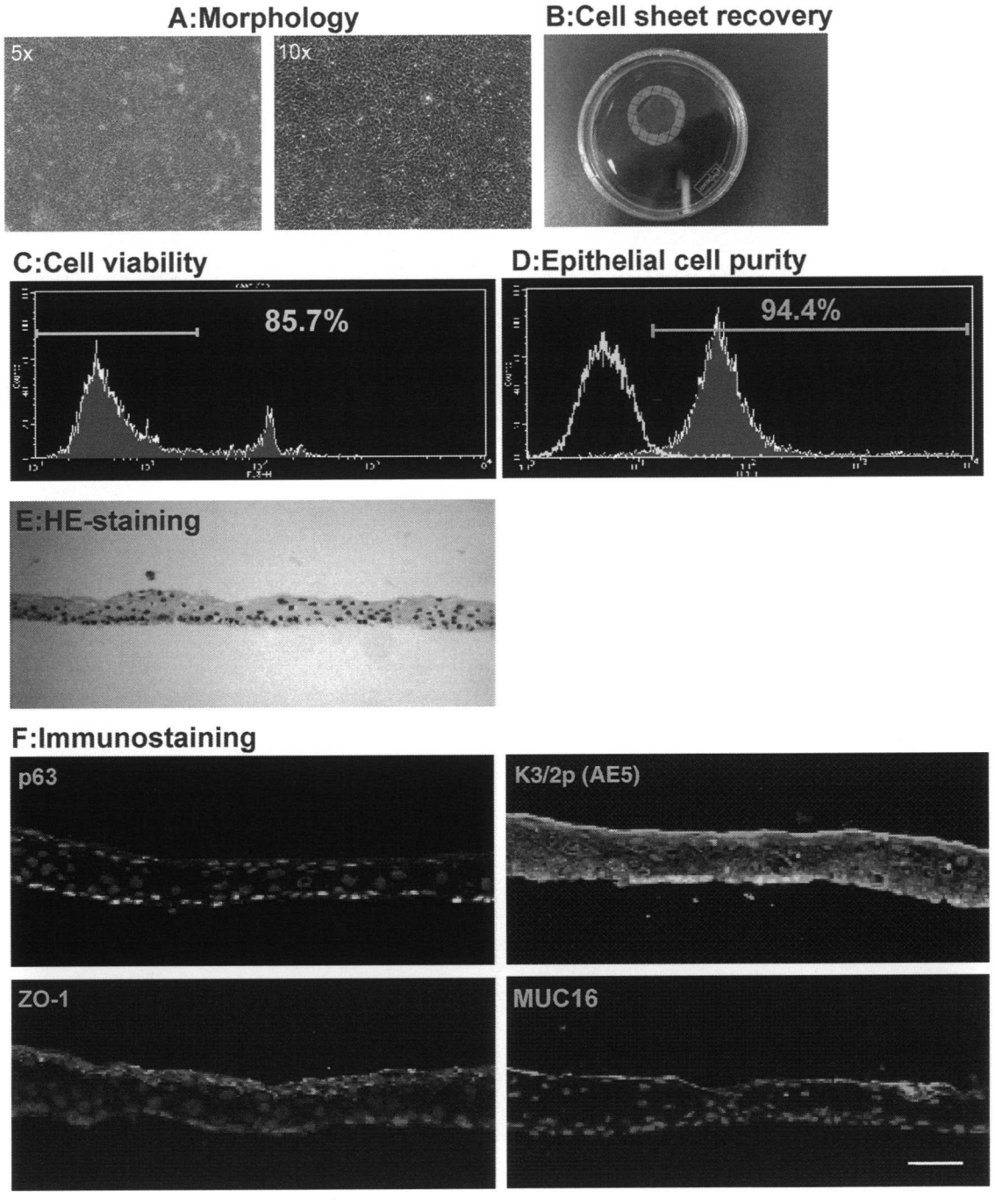

FIG. 5. Validation of human oral mucosal epithelial cell sheets. Human oral mucosal epithelial cells were cultured on temperature-responsive cell inserts for 15 days. Cell morphological examination was performed by phase contrast microscopy (**A**), and then cultured epithelial cells were harvested by reducing temperature to 20°C (**B**). The harvested cell sheet was used for flow cytometric analyses (**C, D**), HE staining (**E**), and immunostaining for p63, K3/2p, ZO-1, and MUC16 (**F**), to validate the quality of cell sheets.

determination of appropriate culture periods before harvest is crucial to fabrication of transplantable cell sheets. In the total cell number determination test, day 28 sheet showed fewer total cell number than day 15 sheet. This indicated that excessive culture period promoted the epithelial cell turnover as phase contrast observation showed, and finally resulted in decrease of total cell numbers. This result corresponded with the result of HE staining, which showed that day 28 sheet had fewer cell layers than day 15 sheet. In addition, the decrease in cell viability in day 28 sheet was also

TABLE 2. SUMMARY OF VALIDATION OF HUMAN CORNEAL AND ORAL MUCOSAL EPITHELIAL CELLS

	Phase contrast	*Detachment test*	*Cell ($\times 10^5$)*	*Viability (%)*	*Purity (%)*	*Stratification (HE)*	*p63*	*K3/2p*	*Muc16 ZO-1*
CO 1	Normal	Possible	10	92.8	97.9	Normal	Posi	Posi	Posi
CO 2	Normal	Possible	11	93.1	95.3	Normal	Posi	Posi	Posi
CO 3	Normal	Possible	8.0	87.1	93.0	Normal	Posi	Posi	Posi
OR 1	Normal	Possible	11	85.7	94.4	Normal	Posi	Posi	Posi
OR 2	Normal	Possible	16	83.3	98.7	Normal	Posi	Posi	Posi
OR 3	Normal	Possible	9.5	89.8	98.1	Normal	Posi	Posi	Posi

CO, human corneal epithelial cell; OR, human oral mucosal epithelial cell; Posi, positive.

caused by excessive cell turnover. These results of day 28 sheet indicated that most of the 3T3 cells did not remain beyond 2 weeks on the culture dish due to mitomycin C treatment, and could no longer support proliferation or maintenance of the epithelial stem/progenitor cells after 2 weeks. In actuality, when the feeder layer was replaced by a new one at the point of day 15, epithelial cells can be maintained without any aberration after additional 14 days culture (data not shown). Interestingly, in the epithelial cell purity analysis and p63 immunostaining, there were no remarkable differences between day 15 and 28 sheets. This result suggested that some defects in day 28 sheets were possibly caused by the loss of the appropriate regulations for proliferation and differentiation of stem/progenitor cells in the additional 2 weeks of culture, rather than the maintenance of stem/progenitor cells by 3T3 cells. In addition, the long culture periods did not promote nonepithelial cell proliferation such as fibroblasts.

We performed the validation not only for the corneal but also for the oral mucosal epithelial cell sheet, because for bilateral corneal disease, we perform transplantation with the cultured epithelial cell sheet fabricated from the patient's own oral mucosal epithelium. The results of each of the three cell sheets showed that there were no remarkable differences between the two epithelial cell sheets. It should be noticed that the ocular surface–specific mucin MUC16, which is not expressed in oral mucosa *in vivo*, was expressed in all three oral mucosal epithelial cell sheets. This corresponded with our previous report,[21] suggesting that this culture condition promoted oral mucosal epithelial cells to express MUC16.

We previously showed that the tissue-engineered epithelial cell sheets that had cultured for 2 weeks were successfully transplanted to patient' eyes and restored their ocular surface.[11] These previous and present results strongly suggested that culturing epithelial cells for around 15 days is the most appropriate for clinical application. Further, our results suggested that among the nine items in the validation system, especially (1) cell morphology, (2) cell recovery, (3) total cell number, and (4) cell viability, in which results were notably different between day 15 sheet and the others, were thought to be the most important factors, and (7) existence of stem/progenitor cells is also an important factor in general for regenerative medicine.

Conclusion

In the present study, our validation system worked well with both corneal and oral mucosal epithelial cell sheets. Using this system, we could standardize the quality of cell sheets for clinical use even in different facilities. This validation system would contribute to the establishment of safe and effective regenerative therapy with cell sheet techniques as a standard therapy.

Acknowledgments

This work was supported in part by the Grants-in-Aid for Scientific Research from the Japan Science and Technology Agency, the High-Tech Research Center Program, and the Formation of Innovation Center for Fusion of Advanced Technologies in the Special Coordination Funds for Promoting Science and Technology from the Ministry of Education, Culture, Sports, Science and Technology, as well as New Energy and Industrial Technology Development Organization (P05008; NEDO), Japan.

Disclosure Statement

No competing financial interests exist.

References

1. Schermer, A., Galvin, S., and Sun, T.T. Differentiation-related expression of a major 64K corneal keratin *in vivo* and in culture suggests limbal location of corneal epithelial stem cells. J Cell Biol **103,** 49, 1986.
2. Cotsarelis, G., Cheng, S.Z., Dong, G., Sun, T.T., and Lavker, R.M. Existence of slow-cycling limbal epithelial basal cells that can be preferentially stimulated to proliferate: implications on epithelial stem cells. Cell **57,** 201, 1989.
3. Lavker, R.M., and Sun, T.T. Epidermal stem cells: properties, markers, and location. Proc Natl Acad Sci USA **97,** 13473, 2000.
4. Tseng, S.C. Concept and application of limbal stem cells. Eye **3,** 141, 1989.
5. Nishida, K. Tissue engineering of the cornea. Cornea **22(7 Suppl),** S28, 2003.
6. Tsubota, K., Satake, Y., Kaido, M., Shinozaki, N., Shimmura, S., Bissen-Miyajima, H., and Shimazaki, J. Treatment of severe ocular-surface disorders with corneal epithelial stem-cell transplantation. N Engl J Med **340,** 1697, 1999.
7. Samson, C.M., Nduaguba, C., Baltatzis, S., and Foster, C.S. Limbal stem cell transplantation in chronic inflammatory eye disease. Ophthalmology **109,** 862, 2002.
8. Ilari, L., and Daya, S.M. Long-term outcomes of keratolimbal allograft for the treatment of severe ocular surface disorders. Ophthalmology **109,** 1278, 2002.
9. Shimazaki, J., Shimmura, S., Fujishima, H., and Tsubota, K. Association of preoperative tear function with surgical outcome in severe Stevens-Johnson syndrome. Ophthalmology **107,** 1518, 2000.

10. Nishida, K., Yamato, M., Hayashida, Y., Watanabe, K., Maeda, N., Watanabe, H., Yamamoto, K., Nagai, S., Kikuchi, A., Tano, Y., and Okano, T. Functional bioengineered corneal epithelial sheet grafts from corneal stem cells expanded *ex vivo* on a temperature-responsive cell culture surface. Transplantation **77,** 379, 2004.
11. Nishida, K., Yamato, M., Hayashida, Y., Watanabe, K., Yamamoto, K., Adachi, E., Nagai, S., Kikuchi, A., Maeda, N., Watanabe, H., Okano, T., and Tano, Y. Corneal reconstruction with tissue-engineered cell sheets composed of autologous oral mucosal epithelium. N Engl J Med **351,** 1187, 2004.
12. Pellegrini, G., Traverso, C.E., Franzi, A.T., Zingirian, M., Cancedda, R., and De Luca, M. Long-term restoration of damaged corneal surfaces with autologous cultivated corneal epithelium. Lancet **349,** 990, 1997.
13. Tsai, R.J., Li, L.M., and Chen, J.K. Reconstruction of damaged corneas by transplantation of autologous limbal epithelial cells. N Engl J Med **343,** 86, 2000.
14. Rama, P., Bonini, S., Lambiase, A., Golisano, O., Paterna, P., De Luca, M., and Pellegrini, G. Autologous fibrin-cultured limbal stem cells permanently restore the corneal surface of patients with total limbal stem cell deficiency. Transplantation **72,** 1478, 2001.
15. Pellegrini, G., Dellambra, E., Golisano, O., Martinelli, E., Fantozzi, I., Bondanza, S., Ponzin, D., McKeon, F., and De Luca, M. p63 identifies keratinocyte stem cells. Proc Natl Acad Sci USA **98,** 3156, 2001.
16. Wang, Y., Chen, M., and Wolosin, J.M. ZO-1 in corneal epithelium; stratal distribution and synthesis induction by outer cell removal. Exp Eye Res **57,** 283, 1993.
17. Hayashida, Y., Nishida, K., Yamato, M., Watanabe, K., Maeda, N., Watanabe, H., Kikuchi, A., Okano, T., and Tano, Y. Ocular surface reconstruction using autologous rabbit oral mucosal epithelial sheets fabricated *ex vivo* on a temperature-responsive culture surface. Invest Ophthalmol Vis Sci **46,** 1632, 2005.
18. Hori, Y., Sugiyama, H., Soma, T., and Nishida, K. Expression of membrane-associated mucins in cultivated human oral mucosal epithelial cells. Cornea **26(9 Suppl 1),** S65, 2007.
19. Nakamura, T., Inatomi, T., Sotozono, C., Amemiya, T., Kanamura, N., and Kinoshita, S. Transplantation of cultivated autologous oral mucosal epithelial cells in patients with severe ocular surface disorders. Br J Ophthalmol **88,** 1280, 2004.
20. Nakamura, T., Inatomi, T., Cooper, L.J., Rigby, H., Fullwood, N.J., and Kinoshita, S. Phenotypic investigation of human eyes with transplanted autologous cultivated oral mucosal epithelial sheets for severe ocular surface diseases. Ophthalmology **114,** 1080, 2007.
21. Hori, Y., Nishida, K., Yamato, M., Sugiyama, H., Soma, T., Inoue, T., Maeda, N., Okano, T., and Tano, Y. Differential expression of MUC16 in human oral mucosal epithelium and cultivated epithelial sheets. Exp Eye Res **87,** 191, 2008.

Address correspondence to:
Kohji Nishida, M.D., Ph.D.
Department of Ophthalmology
Tohoku University Graduate School of Medicine
1-1 Seiryomachi, Aoba-ku
Sendai 980-8574
Japan

E-mail: knishida@oph.med.tohoku.ac.jp

Received: April 23, 2009
Accepted: August 31, 2009
Online Publication Date: November 17, 2009

Annals of Biomedical Engineering (© 2010)
DOI: 10.1007/s10439-010-0035-1

Cell Attachment–Detachment Control on Temperature-Responsive Thin Surfaces for Novel Tissue Engineering

YOSHIKAZU KUMASHIRO, MASAYUKI YAMATO, and TERUO OKANO

Institute of Advanced Biomedical Engineering and Science, Tokyo Women's Medical University (TWIns), 8-1 Kawadacho, Shinjuku, Tokyo 162-8666, Japan

(Received 31 January 2010; accepted 31 March 2010)

Associate Editor Michael S. Detamore oversaw the review of this article.

Abstract—Temperature-responsive intelligent surfaces, prepared by the modification of an interface mainly with poly(*N*-isopropylacrylamide) and its derivatives, have been investigated. Such surfaces exhibit temperature-responsive hydrophilic/hydrophobic alterations with external temperature changes, which, in turn, result in thermally modulated attachment and detachment with cells. The advantage of this system is that cells cultured on such temperature-responsive surfaces can be recovered as single cells and/or confluent cell sheets, while keeping the deposited extracellular matrix intact, simply by lowering the temperature without conventional enzymatic treatment. Here, we focus and compare various methods of producing temperature-responsive surfaces for controlling cell attachment/detachment. Spontaneous cell attachment and detachment using several types of temperature-responsive surfaces are mentioned and various effects, such as film thickness and polymer conformation, are discussed. In addition, the development of the next generation of temperature-responsive surfaces using modifications of the polymer coating to allow for rapid cell recovery is summarized.

Keywords—Temperature-responsive surface, Extra cellular matrix, *N*-isopropylacrylamide, Cell attachment, Cell detachment, Polymeric thin surface.

ABBREVIATIONS

AAc	Acrylic acid
AFM	Atomic force microscopy
ATR-FTIR	Attenuated total reflection-Fourier transform
ATRP	Atom transfer radical polymerization
CIPAAm	2-Carboxyisopropylacrylamide
CS	Coverslips
EB	Electron beam
ECM	Extra cellular matrix
EC	Bovine aortic endothelial cell
EDC	1-Ethyl-3-(3-dimethylaminopropyl) carbodiimide
FN	Fibronectin
HPDL	Human periodontal ligament cells
HUVEC	Human umbilical vein endothelial cells
IPAAm	*N*-isopropylacrylamide
LCST	Lower critical solution temperature
MDCK	Madin-Darby canine kidney
NHS	*N*-hydroxysuccinimide
PEG	Poly(ethylene glycol)
RCO	Rat calvarial osteoblasts
RGD	Arg-Gly-Asp
RGDS	Arg-Gly-Asp-Ser
TCPS	Tissue Culture Polystyrene
ToF-SIMS	Time of flight secondary ion mass spectrometer
XPS	X-ray photoelectron spectroscopy

Address correspondence to Teruo Okano, Institute of Advanced Biomedical Engineering and Science, Tokyo Women's Medical University (TWIns), 8-1 Kawadacho, Shinjuku, Tokyo 162-8666, Japan. Electronic mail: tokano@abmes.twmu.ac.jp

INTRODUCTION

Over the past two decades, tissue engineering utilizing biodegradable scaffolds has pursued its usefulness in order to re-create many organized tissue structures.[16,36] Although its early clinical treatment results in cartilage or urinary bladder have been reported,[9] the clinical applications of tissue engineering based on biodegradable scaffold are extremely limited. The precise reason is that the re-creation of tissue structures requires the development of diffuse vascular networks for providing critical nutrients, such as glucose and oxygen. Furthermore, it seems plausible that biodegradable scaffolds may be unsuitable for the regeneration of cell-dense tissues including

Published online: 13 April 2010

myocardium and hepatic structure.[19,50,58,60,61] Although the degradation of biocompatible and biodegradable polymers such as poly(lactic acid), poly(glycolic acid), and their copolymers theoretically allows proliferating cells to migrate into the space previously occupied by the degraded biomaterials, the large amounts of ECM components are often present within the scaffolding structures. Additionally, significant inflammatory responses are commonly observed due to the degradable products of polymer materials. While this inflammatory response can theoretically induce the recruitment of various leukocytes and possibly direct new blood-vessel formation, host responses to the implanted scaffolds can also potentially damage the cells both within the implanted constructs and in the surrounding host tissues. Based on these observations, tissue-engineering techniques that can re-create adequate blood supplies are essential for properly reconstructed tissues that possess the structure and function of the native organs.[15,37,59,73]

In order to overcome these problems, an innovative approach to tissue engineering using temperature-responsive culture surface has been developed since 1990.[64,70] PIPAAm and its copolymers exhibit a LCST in aqueous media in the vicinity of 32 °C.[20] While they hydrate and form an expanded structure in aqueous media below the LCST, they dehydrate and form a compact structure above the LCST. Such a conformational change in response to temperature has been extensively used to modulate physicochemical properties of polymeric materials.[30,46,47,74] At 37 °C, PIPAAm-grafted surface is slightly hydrophobic, allowing cells to proliferate under normal conditions. A decrease in temperature below 32 °C, however, results in the rapid hydration of the polymer surface, leading to the spontaneous detachment of the cells as a single cell and/or a uniform tissue sheets. As PIPAAm is covalently immobilized onto the culture surfaces, PIPAAm remains bound to the surfaces even after cell detachment. This gives the non-invasive harvest of cultured cells as an intact layer cell sheet containing deposited ECM.[32] The cell sheet can be collected simply by reducing culture temperature lower than 32 °C for less than 1 h, without any enzymes such as trypsin. This technology allows us to transplant cell sheets to host tissues without using biodegradable scaffolds (Fig. 1).

Using cell sheet engineering we can altogether avoid to use scaffolds, and to fix and suture them for conventional tissue engineering approaches using isolated cell injections and scaffold-based technologies whose applicability is often limited. The direct transplantations have been applied to corneal epithelia,[48,49] periodontal ligament cells,[26] myoblast cells,[42] and esophageal epithelia.[51]

In this review, the fundamental mechanism of cell attachment and detachment on temperature-responsive polymeric surface in response to temperature is summarized. Especially, we focused on several topics, (1) the effects of polymer conformation toward cell attachment and detachment on temperature-responsive surfaces, (2) the detailed mechanism of cell detachment from temperature-responsive surfaces with preserving ECM components beneath a single cell and

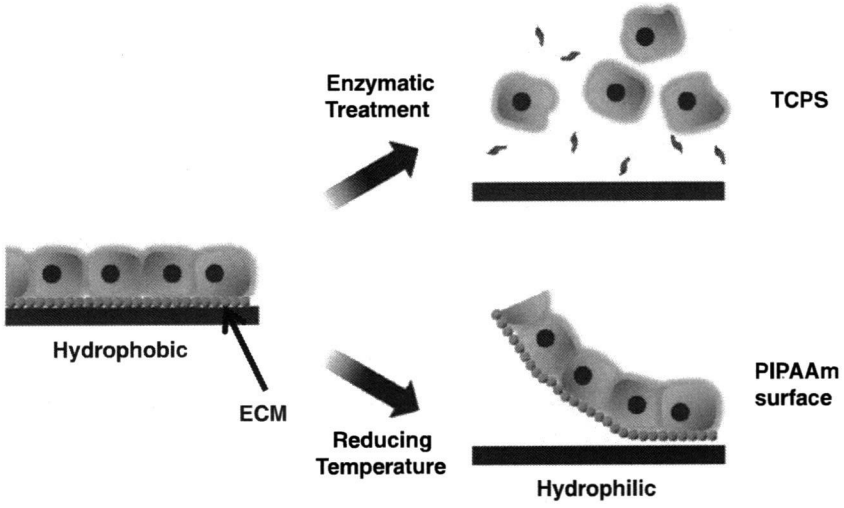

FIGURE 1. Cell sheet harvested from PIPAAm-grafted surfaces. Cells can attach and proliferate onto temperature-responsive surfaces at 37 °C, whereas lowering temperature to 20 °C facilitates the detachment of cell layers as a cell sheets. In the case of tissue culture polystyrene surfaces, enzymatic treatment, which is necessary for the harvesting of cells, damages cell–cell connections and the deposited ECM.

a cell sheet, (3) the acceleration of cell detachment from temperature-responsive surfaces controlled by the modification of temperature-responsive surface, and (4) the affinity control mechanism of novel cell culture surfaces.

EFFECTS OF POLYMER CONFORMATION TOWARD CELL ATTACHMENT AND DETACHMENT ON TEMPERATURE-RESPONSIVE SURFACES

A conventional culture method was used for growing confluent cells on the surface of a TCPS surface. Cells were then harvested by the enzymatic proteolysis of ECM with trypsin or other proteolytic enzyme, and by chelating Ca^{2+} ions to disrupt cell–cell junctions with ethylenediamine tetraacetic acid.[4,66] PIPAAm-grafted TCPS surface as a temperature-responsive culture substrate have been developed since 1990 allowing cultured cells to be recovered simply by lowering temperature.[55,70] Temperature-responsive polymers have been widely used as a substrate not only for single cell recovery but also for engineering cell sheets as mentioned above. Over the years, many different types of cells and substrates have been investigated, as the methods of grafting PIPAAm to surfaces have been developed.[10]

Takezawa *et al.* have reported cell cultures on TCPS coated with a mixture of PIPAAm and collagen since 1990.[64,65] Neither adhesion nor proliferation of fibroblasts was observed on TCPS coated with only PIPAAm, whereas cells adhered and proliferated on TCPS coated with a mixture of PIPAAm and collagen. These results imply that fibroblasts cannot adhere and proliferate on coatings composed solely PIPAAm without the affinity interactions of collagen, because free PIPAAm chains are released into the solution from hydrophobic polystyrene surfaces. These data prove that the graft architecture and thickness of PIPAAm immobilized covalently on TCPS both play a crucial role in the temperature-induced alterations of hydrophilic/hydrophobic properties and cell adhesion/detachment.

In our preliminary studies, the grafted amounts of PIPAAm on surfaces also have a significant influence on cell adhesion behavior.[70] The correlation of the thickness of PIPAAm covalently grafted layer on TCPS surfaces and cell adhesion/detachment behavior was studied by Akiyama *et al.*[1,29] For this purpose, limited excimer laser ablation and AFM methods for determining the thickness of PIPAAm grafted layers were used.

Two types of PIPAAm-grafted TCPSs were evaluated for the grafted amounts of PIPAAm surfaces and their temperature-responsive wettability changes.[1] From ATR/FT-IR measurements, the grafted polymer amounts on two PIPAAm-grafted surfaces were determined to be 1.4 ± 0.1 $\mu g/cm^2$ ($n = 4$, PIPAAm-1.4-TCPS) and 2.9 ± 0.1 $\mu g/cm^2$ ($n = 4$, PIPAAm-2.9-TCPS), respectively. AFM images clearly show the section profiles of their ablated domains with the UV excimer laser for PIPAAm-1.4-TCPS (Fig. 2a) and for PIPAAm-2.9-TCPS (Fig. 2b). Section profiles showed the depth to be 15.5 ± 7.2 nm, indicating the thickness of grafted PIPAAm layer of PIPAAm-1.4-TCPS. Likewise, the averaged thickness of PIPAAm-grafted layers of PIPAAm-2.9-TCPS was 29.3 ± 8.4 nm. Bovine endothelial cells (ECs) adhered and spread on the PIPAAm-1.4-TCPS surfaces (Fig. 2e), whereas those on PIPAAm-2.9-TCPS failed to do (Fig. 2f). Adhering and proliferating cells on PIPAAm-1.4-TCPS surfaces were detached from the surfaces by reducing temperature below the PIPAAm's transition temperature as a single cell and/or a layered cell sheet depending on cell density on the surfaces.

Cell attachment/detachment control on PIPAAm layer grafted to the glass coverslips was recently performed by Fukumori *et al.*[17] When the monomer concentration was 5 wt.% at EB irradiation for synthesizing PIPAAm-grafted coverslips (PIPAAm-CSs), the grafted polymer density was 0.84 $\mu g/cm^2$ (the film thickness: 3.5 nm observed by AFM, PIPAAm-0.84-CS, Fig. 2c), and cells adhered and spread on the surface at 37 °C, but detached at 20 °C (Fig. 2g). In contrast, when the monomer concentration was 35 wt.%, the polymer density was 1.28 $\mu g/cm^2$ (the film thickness: 7.6 nm, PIPAAm-1.28-CS, Fig. 2d), and the surfaces were cell repellent even at 37 °C (Fig. 2h). These results show a remarkable contrast to those obtained from PIPAAm-grafted TCPS, since various types of cells showed temperature-dependent cell adhesion/detachment, when the grafted density was around 2 $\mu g/cm^2$ on these surfaces.

PIPAAm chains at the outermost surfaces also suffer from progressive dehydration, and consequently ECM, such as FN, should be adsorbed on the surfaces for preparing thin layer, but there is much less progressive dehydration at the outermost surfaces, and as a result, the surfaces become cell repellent due to the thicker layer. For glass surfaces, the poor dehydration of the grafted PIPAAm chains at the interface of the glass is expected, like hydrophobic TCPS surface, due to the presence of remaining hydrophilic silanol groups. To compensate for this drawback, a denser, thinner layer of grafted PIPAAm may be necessary to promote the restriction of molecular motion of the grafted PIPAAm chains and to exhibit cell attachment/detachment properties in response to a change in temperature. The fact that cell attachment/detachment

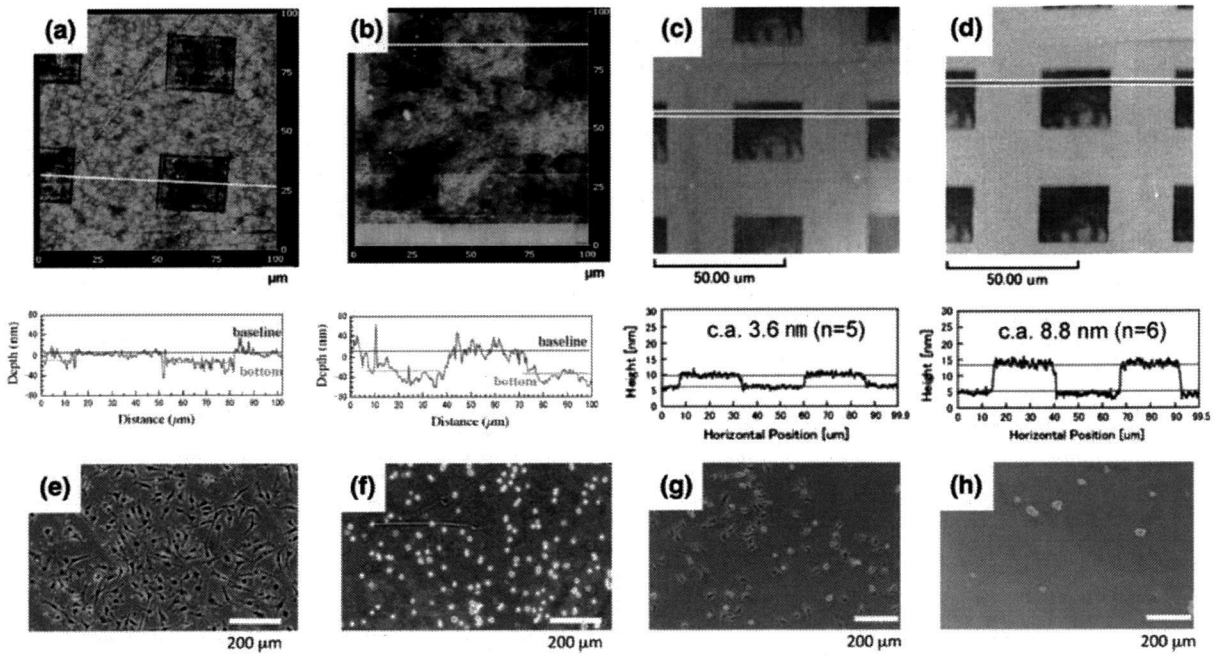

FIGURE 2. Tapping mode AFM observation for laser-ablated domains on (a) PIPAAm-1.4-TCPS, (b) PIPAAm-2.9-TCPS, (c) PIPAAm-0.84-CS, and (d) PIPAAm-1.28-CS surfaces. The baseline and the bottom were the averages of the text data from the section profiles. The scan size was 100 μm × 100 μm. Phase-contrast microphotographs of ECs cultured on (e) PIPAAm-1.4-TCPS, (f) PIPAAm-2.9-TCPS, (g) PIPAAm-0.84-CS, and (h) PIPAAm-1.28-CS surfaces at 37 °C for 1 day. Adapted from Akiyama *et al.*[1] Copyright 2004, American Chemical Society.

controllable PIPAAm layer of PIPAAm-CS is thinner than that of PIPAAm-TCPS is suggestively a result of remaining silanol groups and the greater density of the grafted PIPAAm layer.

The other covalently bonded temperature-responsive surface is synthesized by the plasma polymerization of IPAAm.[8,56] The thickness, elasticity modulus of the surface could be controlled by depositing condition. XPS and ToF-SIMS results revealed that PIPAAm was covalently bonded to the surface. The sum frequency generation results showed that the hydrophobic isopropyl side moieties were oriented at the outermost surface above the LCST, while the disordering structure of isopropyl moieties from vertical of the surface. The cell attachment/detachment studies showed no obvious difference among the different batches of plasma-deposited coatings, even among the different thickness.[5,6] This result suggests that cell attachment/detachment may be insensitive to the grafted layer thickness of plasma-polymerized PIPAAm substrates, but it may be sensitive to the conformational change of the polymeric surface.

Another temperature-responsive surface was synthesized by a copolymer consisted of IPAAm and 4-(*N*-cinnamoylcarbamide)methylstyrene on TCPS, followed by crosslinking the copolymer through the dimerization of the cinnamoyl groups.[67] The thickness of PIPAAm crosslinked surface with the density (2.4–6.9 μg/cm^2) was not dominant factor toward cell adhesion and proliferation.

In the study of Matsuda's group, no ECs adhered to pure PIPAAm or a mixed coating of PIPAAm and gelatin.[22,41,52] Complete cell adhesion and spreading were found on a surface coated with a mixture of PIPAAm–gelatin (20.8 μg/cm^2) and PIPAAm (416 μg/cm^2), which was found to be an optimal ratio for cell attachment. They also found that smooth muscle cells attached to and proliferated on surfaces with PIPAAm-to-gelatin ratio higher than 12:1, which results in mechanically strong, stiff gels, regardless of the concentration of PIPAAm–gelatin. They concluded that a ratio of at least 12:1 and low concentration of PIPAAm–gelatin should be dominant for controlling cell attachment, proliferation, and detachment.[53]

In recent years, novel grafting methods have been developed to prepare well-defined polymer brush layers on surfaces. ATRP, which is a controlled polymerization technique, is an attractive polymer grafting method, because it enables the preparation of surfaces with dense polymer brushes from surface-immobilized ATRP initiators. The dense polymer brush layers exhibit specific properties different from

the dilute brush layers prepared by conventional grafting approaches.[23,24,44,45]

Alexander *et al.* synthesized PIPAAm brushes by ATRP within micropatterned domains at surfaces and discussed the performance of these functionalized surfaces in short-term bioadhesion assays under varying conditions.[2,27] The polymer brushes showed temperature-dependent behavior on surfaces as demonstrated by changes in contact angle, surface energy components, and aqueous phase AFM. The responses in the polymer brush domains resulted in temperature-controlled attachment of bovine serum albumin, and the common oral bacteria *Streptococcus mutans*.[2]

Mizutani *et al.* prepared PIPAAm brushes on poly(4-vinylbenzyl chloride)-coated polystyrene surfaces using surface-initiated ATRP and applied these to temperature-responsive cell culture substrates in 2008.[43] The surface characteristics of PIPAAm brushes in relation to ECs attachment/detachment were controlled by the PIPAAm layer thickness. Though ECs can be adhered at 37 °C for the thinner surface with less than 30 nm PIPAAm thickness, cell is unable to attach on the thicker surface. By adjusting the polymerization reaction conditions and time, polymer layers supporting confluent cultures of ECs were possible, indicating that PIPAAm brush surfaces prepared by surface-initiated ATRP techniques give surface selection in the preparation of cell sheets from attachment-dependent cells with a relatively strong adhesive property for tissue engineering applications.

MECHANISM OF CELL DETACHMENT FROM TEMPERATURE-RESPONSIVE SURFACES

The mechanism of cell detachment is one of the most important aspects of cell sheet engineering. Cell detachment from temperature-responsive surfaces has been investigated using PIPAAm as a substrate.[54] A two-step mechanism was proposed by our group in 1995. First step is a passive step, where cell detachment is induced by the hydration of PIPAAm chains on the substrate, followed by an active step involving cells' shape change and detachment from the surface driven by cytoskeletal action and metabolic processes. Firstly, cells attached to the surface at 37 °C, followed by the proliferation. Immediately after reducing temperature, the cells' morphology was less spread, and the cell started to detach. The detachment continues until the cells no longer have a spread and flattened morphology. The schematic depictions of the shape changes that cells undergo are shown in Fig. 3a.

Detachment seems also to be mediated by active cellular metabolic processes and cell detachment can be suppressed by adding an ATP synthesis inhibitor.[71] Selective inhibition of actin filaments, by means of either an actin stabilizer or an actin depolymerizer,

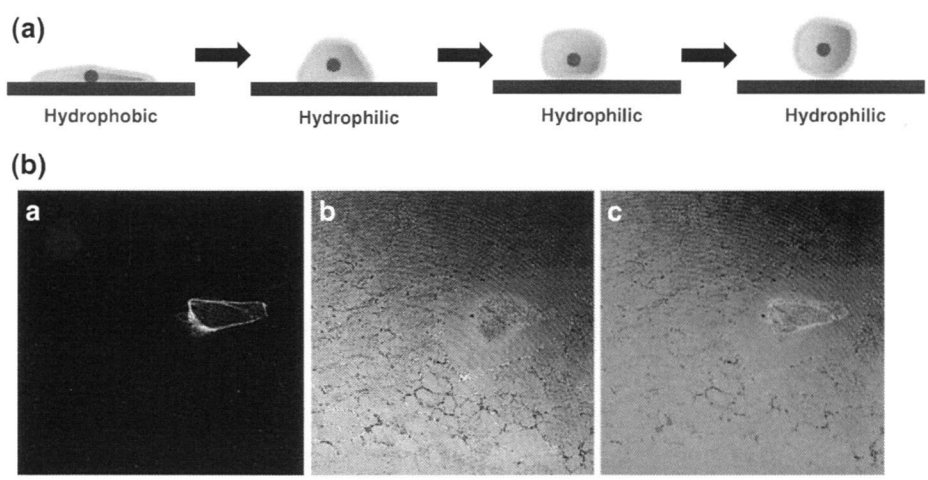

FIGURE 3. (a) Schematic representation showing the mechanism of cell sheet detachment from PIPAAm surfaces. (b) Confocal laser scanning microscopy of bovine aortic endothelial cells detaching from a PIPAAm-grafted TCPS surface. ECs were plated on a PIPAAm-grafted surface in the presence of serum and cultured for 6 h at 37 °C. Then temperature was reduced to 20 °C. Shrinking cells were fixed, stained with rhodamine-phalloidin, and observed by a confocal laser scanning microscope. The obtained fluorescence image (a and red in c) and interference reflection image (b and green in c) were superimposed. F-actin was observed to remain organized inside the cells as peripheral rings even during the detachment process. Interference reflection microscopy revealed small deposits on the surfaces. Some deposits were organized into networks. Since deposits were unable to be observed prior to cell culture, serum proteins such as FNs were presumed to be deposited onto the surfaces. However, small smooth areas without such deposits were observed only in the vicinity of shrinking and rounding cells. The outlines of the smooth areas highly resembled that of shrinking cells, implying that the formerly flattened and spread cell occupied the same smooth area before reducing temperature. Adapted from Yamato *et al.*[71] Copyright 2000, Elsevier.